Heliyon 5 (2019) e02759

Contents lists available at ScienceDirect

Heliyon

journal homepage: www.heliyon.com

Research article

Quantum chemical and experimental evaluation of the inhibitory action of two imidazole derivatives on mild steel corrosion in sulphuric acid medium

M. Ouakki [a], M. Galai [b,*], M. Rbaa [c], A.S. Abousalem [d,e], B. Lakhrissi [b], E.H. Rifi [f], M. Cherkaoui [a]

[a] Laboratory of Materials, Electrochemistry and Environment (LMEE), Faculty of Sciences, Ibn Tofail University, PB. 133-14000, Kenitra, Morocco
[b] Laboratory of Materials Engineering and Environment: Modelling and Application (LMEEMA), Faculty of Sciences, Ibn Tofail University, PB. 133-14000, Kenitra, Morocco
[c] Laboratory Agro-Resources, Polymers and Process Engineering, Faculty of Sciences, Ibn Tofail University, PB. 133-14000, Kenitra, Morocco
[d] Chemistry Department, Faculty of Science, Mansoura University, El-Mansoura, 35516, Egypt
[e] Quality Control Lab, Operation Department, Jotun, Egypt
[f] Laboratory of Organic Synthesis and Extraction Processes (LOSEP), Faculty of Sciences, Ibn Tofail University, PB. 133-14000, Kenitra, Morocco

ARTICLE INFO

Keywords:
Materials chemistry
Electrochemistry
Theoretical chemistry
H_2SO_4
Corrosion inhibition
DFT
Adsorption
Imidazole
EIS

ABSTRACT

The adsorption and corrosion inhibition properties of two imidazole derivatives namely, 2-(4-chlorophenyl)-1,4,5-triphenyl-1H-imidazole (IM-Cl) and 1,4,5-triphenyl-2-(p-tolyl)-1H-imidazole (IM-CH_3) for mild steel in 0.5 M H_2SO_4 solution are studiedby electrochemical and computational calculations. The results obtained from the electrochemical methods show that IM-Cl and IM-CH_3imparted high resistance and behave as mixed type inhibitors. Inhibition efficiency (IE %) increases with the increase of inhibitors concentration to attain 96 % and 91% at 10^{-3} M of IM-Cl and IM-CH_3 respectively. EISdatais analyzed to model the inhibition process through appropriate equivalent circuit model. Thermodynamic and kinetic parameters controlling the adsorption process are calculated and discussed. DFT calculations are carried out at the B3LYP levels of theory with 6-31G (d,p) basis stein gas and aqueous phase for neutral and protonated forms. Quantum chemical calculations section of the study provides enough calculation and discussion on the relationship between corrosion inhibition and global reactivity descriptors.

1. Introduction

Nowadays, the use of mild steel is widespread because of its excellent structural and mechanical properties [Ouakki et al., 2018a,b]. Considering that acid solutions are also extensively used in the industry for acid pickling processes, ore production, boiler cleaning, industrial cleaning, acid descaling and petrochemical processes [El Faydy et al., 2018; Singh et al., 2016; Haque et al., 2017; Zhai et al., 2016]. Many metallic installations have suffered serious deterioration due to the aggressive nature of these acid solutions. Various corrosion protection methods are used to reduce its attack on the metallic materials.

Several methods of corrosion protection have been considered so far by several authors [Gasiorek et al., 2018]. These methods can be classified into those that modify the potential of the electrode on the metal surface or those thatmodify the nature of the metal itself. Cathodic protection and anodic protection aretwo methodsof corrosion control by changing the electrode potential [McCafferty, 2010; Kautek, 1988].

The nature of the metal can be modified by the use of metal coatings (sacrificial or noble) or by the choice of a material from which a morecorrosion-resistant alloy is selected rather than a less corrosion-resistant alloy. However, most frequently, the choice of materials is not an option because of the need to maintain other desirable properties (such as mechanical strength), or is prohibited by cost. In such cases, the modification of the environment by the use of corrosion inhibitors becomes a possible means of corrosion control [Abdullah Dar, 2011]. However, the use of corrosion inhibitors has been found to be themosteffective and thecheapest method for protection and prevention of steel [Tebhji et al., 2005]. Generally, the inhibitors caninteractwith either anodic or cathodic corrosion reactions or/and form protective layers through adsorption onto the steel surface. The most efficient and effective corrosion inhibitors are organic compounds containing functional electronegative groups, π-electrons, in conjugated double or triple bonds or aromatic rings. There is also a specific interaction between functional groups containing hetero atoms like nitrogen, sulfur, oxygen, having free

* Corresponding author.
E-mail address: galaimouhsine@gmail.com (M. Galai).

https://doi.org/10.1016/j.heliyon.2019.e02759
Received 9 November 2018; Received in revised form 20 August 2019; Accepted 28 October 2019

Table 1
List of imidazole compounds used as corrosion inhibitors on corrosion of steel in acidic medium.

Structure of inhibitor	IUPAC name	Metal	Electrolyte
A	2-methyl-4-phenyl-1-tosyl-4, 5-dihydro-1H-imidazole [Zhang et al., 2015]	P110 carbon steel	1 M HCl
B	N-vinylimidazolemonomer [Zhang et al., 2015]	Stainless steel	1N H_2SO_4
C	poly-N-vinylimidazole [Öncül et al., 2011]	Stainless steel	1N H_2SO_4
D	2-(1-(morpholinomethyl)-1Hbenzo[d] imidazol-2-yl)phenol (MBP) 2-(1-((piperazine-1-yl)methyl)-1H-benzo[d]imidazol-2-yl)phenol (PzMBP) 2-(1-((piperidine-1-yl)methyl)-1H-benzo[d]imidazol-2-yl)phenol (PMBP) [Yadav et al., 2016]	N80 steel	15% HCl

lone pair of electrons and the metal surface, which play an important role in inhibition. When two of these featuresare combined, increased inhibition can be observed [Moradi and Attar, 2014; Shivakumar and Mohana, 2012; Galai et al., 2017]. Recently many researchers have reoriented their attention to the useof new organic compounds as corrosion inhibitors such aspyrazole [Hammouti et al., 1995; Aouniti et al., 1998; El-Ouafi et al., 2002], triazole [Salghi et al., 2000; Bentiss et al., 1999], Triazepine Carboxylate [Alaoui et al., 2018], tetrazole [Kertit and Hammouti, 1996; Kertit et al., 1998], imidazopyridine [Ech-chihbi et al., 2016; Ech-chihbi et al., 2017] and imidazole [Galai et al., 2016; Rbaa et al., 2017a,b]. Recently, imidazole has attracted a lot of attention in the field of metallic corrosion inhibition due to their interesting properties, low cost and their ease of synthesis [Verma et al., 2018]. Imidazole derivatives have been evaluated as effective corrosion inhibitors in various media by several investigators. Table 1 and Fig. 1 displays some imidazole compounds used as corrosion inhibitorson corrosion of steel in acidic medium.

Most organic compounds inhibit corrosion via adsorption on the metal surface. This adsorption mainly depends on some physico-chemicalproperties of the molecule, related to its functional groups (e.g. nitrogen, oxygen and sulfur atoms), aromaticity, the possible steric effects and electronic density. The aim of this work is to study the inhibition properties of two imidazole derivatives on mild steel corrosion in 0.5 M H_2SO_4 using gravimetric measurements, potentiodynamic polarization curves, and electrochemical impedance spectroscopy. It also aimsto predict the thermodynamic feasibility of these compounds on the steel surface. In addition, detailed investigation of temperature were also carried and discussed to improve a better understanding of the adsorption mechanism of the studied inhibitors.

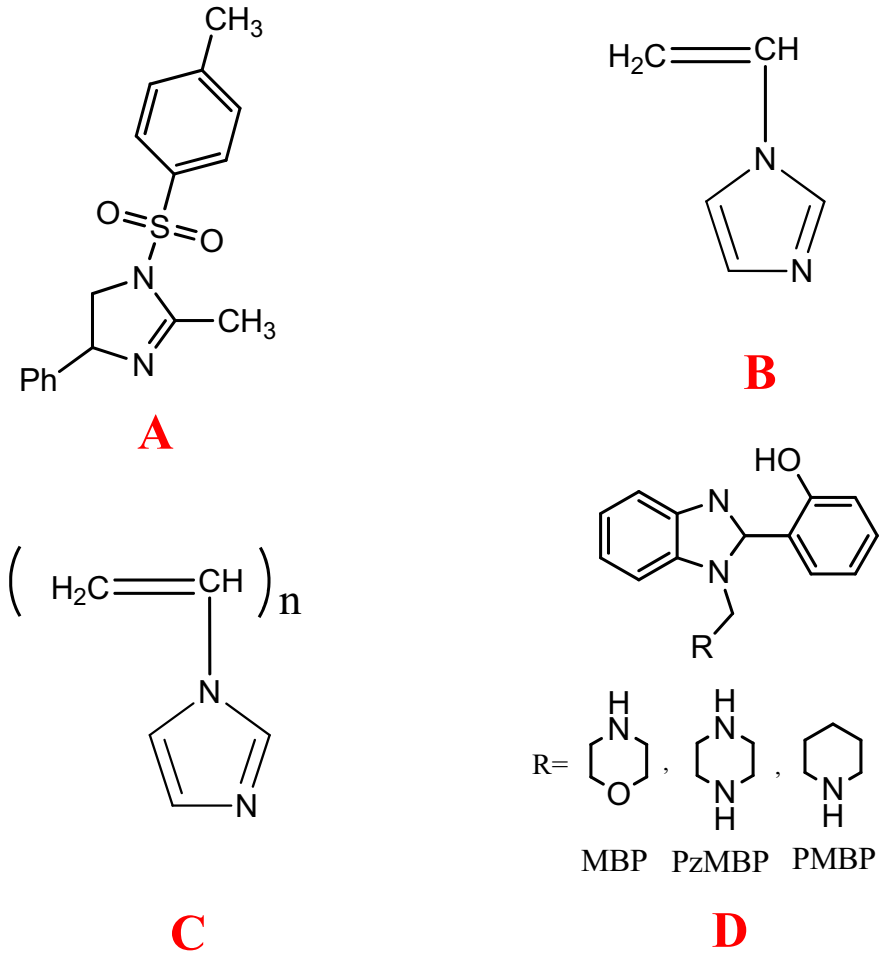

Fig. 1. Imidazole compoundsand some of its derivatives usedfor corrosion inhibition of mild steel in acid medium: (A) 2-methyl-4-phenyl-1-tosyl-4, 5- dihydro-1H-imidazole, (B) N-vinylimidazolemonomer, (C) poly-N-vinylimidazole and (D) 2-(1-(morpholinomethyl), 1Hbenzo[d]imidazol-2-yl)phenol (MBP), 2-(1-((piperazine-1-yl)methyl)-1H-benzo[d]imidazol-2-yl)phenol (PzMBP), 2-(1-((piperidine-1-yl)methyl)-1H-benzo[d]imidazol-2-yl)phenol (PMBP).

Table 2
Names, chemical structures and abbreviations of the studied Imidazole compounds.

Inhibitor code	Molecular structures/chemical names	Mol formulas (F.wt)
IM-Cl	2-(4-chlorophenyl)-1,4,5-triphenyl-1H-imidazole	$C_{27}H_{19}N_2Cl$ (406,90 g/mol)
IM-CH_3	1,4,5-triphenyl-2-(p-tolyl)-1H-imidazole	$C_{28}H_{22}N_2$ (386,48 g/mol)

2. Materials & methods

2.1. Materials and sample preparation

The aggressive medium (0.5 M H_2SO_4)was prepared by dilution of analytical grade H_2SO_4 (98 wt.%) with distilled water. The concentrations of imidazole derivatives inhibitors in the work were set as 10^{-6} to10^{-3}M and the blank solution was also prepared for comparison. Mild steel samples (0.17 wt.% C, 0.37 wt.% Mn, 0.20 wt.% Si, 0.03 wt.% S, 0.01 wt.% P and balance Fe) were cut into 2.00 cm * 1.00 cm * 0.20 cm for weight loss tests. For electrochemical experiments, the steel samples were used with an exposed surface of 1.0 cm^2 to the acid solution. Prior to use, the steel samples were prepared by polishing with emery paper at different grit sizes (from 180 to 2000), cleaned with distilled water and ethanol, and dried in room temperature. The chemical structures of the studied inhibitors are shown in Table 2 and Fig. 2.

2.2. Weight loss experiments

The weight loss experiments were achieved using the standard method described earlier [Gupta et al., 2016a,b]. The corrosion rate was calculated using the following Eq. (1):

$$CR = \frac{W}{St} \tag{1}$$

Where, W is the weight loss of mild steel sample, S is the area of mild steel sampleand t is theimmersion time (6 h).

The inhibition efficiency, η_{CR}%, is determined according to the-following Eq. (2)

$$\eta_{CR\%} = \frac{CR - CR_{inh}}{CR} \times 100 \tag{2}$$

where CR and CR_{inh} are the corrosion rates in the absence and presence of theinhibitors, respectively.

2.3. Electrochemical measurements

Electrochemical measurements were carried by the method described previously [Gupta et al., 2016a,b]. The electrochemical impedance measurements (EIS) were performed on mild steel samplesat constant potential (OCP) in the frequency range from 100 kHz to 100 mHz under potentiostatic conditions using an AC signals with amplitude of 10 mV peak to peak. The charge transfer resistance was calculated from Nyquist plot from which corrosion inhibition efficiency was calculated using the following Eq. (3) [Hermas and Morad, 2008]:

$$\eta_{imp\%} = \frac{R_p - R_p^{\circ}}{R_P} \times 100 \tag{3}$$

$$\theta = \frac{R_p - R_p^{\circ}}{R_P} \times 100 \tag{4}$$

Where R^0_p and R_p are the charge transfer resistance values in the absence and presence of the inhibitors, respectively and θthesurface coverage, given by Eq. (4).

The Potentiodynamic polarization studies were performed on mild steel specimens by automatically changing the electrode potential from −900 to -100 mV/Ag/AgCl versus OCP at a scan rate of 1 mVs^{-1}. The corrosion current density (i_{corr}) was calculated by extrapolating the linear Tafel slopes of anodic and cathodic curves with referenceto the corrosion potential. The inhibition efficiency was determined by using the following Eq. (5) [Liu et al., 2009]:

$$\eta_{pp\%} = \left(\frac{i^{\circ}_{corr} - i_{corr}}{i^{\circ}_{corr}}\right) \times 100 \tag{5}$$

where $i^0_{corr}$and i_{corr} are the corrosion current densities values in the absence and presence of theinhibitor, respectively.

2.4. Surface characterization by SEM/EDX

The determination of the nature of the formed film on the surface of the metal, exposed to 0.5 M H_2SO_4 solution during 6h in theabsence and presence of the studied inhibitors, was realized by Scanning Electron Microscopy (Quanta FEG 450) coupled with EDX analyses. These analyses were performed in foundationMAScIR.

2.5. Computational details

For the theoretical study, quantum chemical calculations were performed for IM-Cl and IM- CH_3 to carry out the optimized geometry using Gaussian 09 software [Sasikumar et al., 2015; Bedair et al., 2017]. The molecular structures in the ground state are optimized and the structural parameters have been computed using density functional theory (DFT). Theoretical calculations were performed with the hybrid B3LYP functional, i.e., a combination of the Becke's three parameters potential with the hybrid correlation functional of Lee-Yang-Parr using 6-31G (d,p) basis set level.

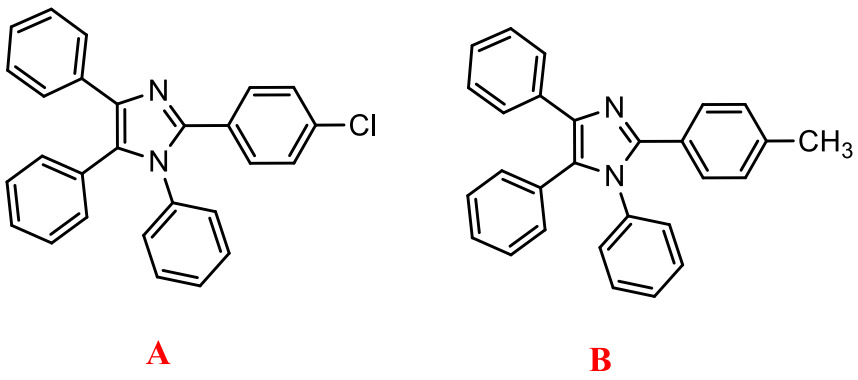

Fig. 2. Chemical structures of IM-Cl (A) and IM-CH_3(B).

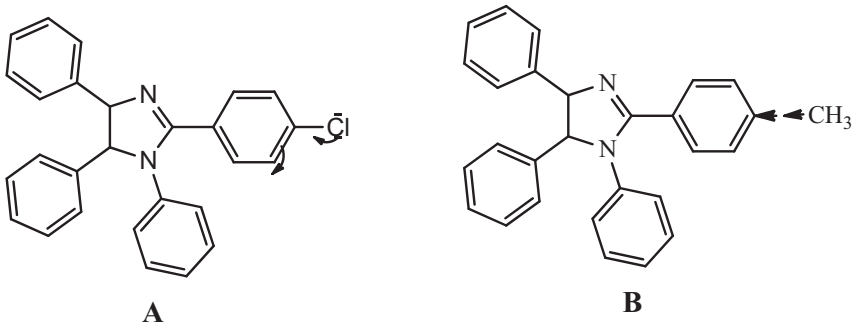

Fig. 3. Mesomeric effect and inductive effect of compounds IM-Cl (A) and IM-CH_3 (B).

The spatial distribution of the HOMO, LUMO, and Electrostatic Potential (ESP) maps are important to understand the adsorption preferences of the inhibitors [Lee et al., 1988; Becke, 1993; Parr and Yang, 1989]. The corresponding quantum chemical descriptorsof molecules both in gas and aqueous phase for neutral and protonated forms were calculated including E_{HOMO}, E_{LUMO}, Energy gap, chemical hardness, softness, electronegativity and chemical potential. Theseare highly effective and useful tools in corrosion studies of metals. Other parameters describing the local selectivity such as the local charge populations and the condensed Fukui functions are also considered.

2.6. Molecular dynamic simulation

As part of the computational chemical studies, Materials Studio software was used to carry out the MD simulation via the application of Monte Carlo simulations [Fouda et al., 2017a,b]. This method find practical importance in corrosion inhibition studies because it predicts the interaction mode of inhibitor molecules on the Fe (1 1 0) surface [Fouda et al., 2017a,b]. In this simulation process, the pure Fe crystal was used and cleaved along (1 1 0) surface plane with a vacuum slab of 30 Å. The Fe (1 1 0) surface was first allowed to relaxation and then, enlarged to a (10 × 10) super cell. This provides a sufficient surface area for the interaction of inhibitor on metal surface. In order to make the MD simulation closer to the real system, a simulation box with dimension of 24.82 × 24.82 × 42.25 $Å^3$ contains 271 H_2O, 6 H_3O, 3 $SO_4^{2-}$and 1 inhibitor molecule was created. The simulations were undertaken in through the adsorption locator tool implemented in Material Studio software with COMPASS force field. Insights on the adsorption of the tested inhibitors and Fe (1 1 0) surface were determined by the calculation of the interaction energies.

3. Results and discussion

3.1. Effect of substitution

The IM-CH_3 molecule has a negative value of the constant Hammett constant σp (- CH3; σp = - 0,17) compared to the other substituents studied {(Cl; σp = 0,23, H; σp = 0, 0)}. This negative value has the electron donor capacity for the IM-CH_3 molecule in organic solvents.

But in our case we worked in an acid medium (H_2SO_4) that affects the molecular structure by protonation. Generally in the acidic medium the mesomeric effect comes into play instead of substituting Hammett. The chlorine group (Cl) is an electron donor by mesomeric effect (+M). On the other hand, the methyl (CH_3) group is an electron donor by inductive effect (+I) Fig. 3. The mesomeric effect of chlorine creates an electrostatic/magnetic field that produces the molecule that promotes the adsorption of the chlorine molecule on the surface of the steel.

3.2. Gravimetric measurement

Thecorrosion rate and inhibition efficiencies obtained from the gravimetric experiments in the presence of different concentrations of inhibitors in 0.5 M $H_2SO_4$are presented in Table 3. The observed weight-loss values of triplicate measurements are highly reproducible giving standard deviations. The resultsshow that the mild steel corroded severely in the uninhibited 0.5 M H_2SO_4 solution, whereas the presence of inhibitors reduced the dissolution rate considerably. Shahin et al. pointed out in their work [Shahin et al., 2002] that the relative inhibition efficiencies of the studied compounds can be rationalized qualitatively under the assumptions that:

Table 3
Corrosion rate (C_R) Values and inhibition efficiency η_{CR} (%)of mild steel in 0.5 M H_2SO_4obtained from gravimetric measurementsat 298 K.

Medium	Concentration (M)	C_R (mg/cm^2.h)	η_{CR} (%)
H_2SO_4 0.5 M	–	10.53 ± 0.1	-
IM-Cl	10^{-6}	1,469 ± 0.03	86,0
	10^{-5}	1,422 ± 0.02	86,5
	10^{-4}	0,851 ± 0.03	91,9
	10^{-3}	0,350 ± 0.01	96,7
IM-CH_3	10^{-6}	1,969 ± 0.02	81,3
	10^{-5}	1,722 ± 0.04	83,6
	10^{-4}	1,451 ± 0.01	86,2
	10^{-3}	0,848 ± 0.08	91,9

- ✓ The corrosion inhibitionis essentially based on the coverage of the metal surface by the inhibitor molecules, thus making the contact of the corrosive mediumdifficult;
- ✓ Attachment of the molecules on the metal surface is facilitated through the coordination of π-electron system to the metal atom;
- ✓ The stability of the complex formed at the metal/solution interface is somewhat related to the molecule's being planar.

Both IM-Cl and IM- CH_3 exhibited substantial protection efficiency for mild steel in 0.5 M H_2SO_4. As the concentration of the inhibitor is increased $\%\eta_{CR}$ also increases. At higher concentration, Maximum inhibition efficiencies of 96.7% and 91.9% were observed for IM-Cl and IM-CH_3respectively at 10^{-3} M. The $\%\eta_{CR}$ is almost leveled off and only slight variation is observed. This can be explained bythe adsorption of the IM-Cl and IM- CH_3onto mild steel surface resulting in the blocking of the reaction sites. The increase in concentration of the inhibitor leads to the gradual formation of multilayers that further reduce the rate of corrosion from the attack of the corrosion active ions in the acid medium beyond what can be achieved with mono layer coverage below that concentration [Amin et al., 2009].

3.3. Electrochemical studies

3.3.1. Open circuit potential

The variances of OCP of the mild steel as a function of time in aerated H_2SO_4 0.5 M solution, in the absence and presence of different concentrations of IM-Cl and IM-CH_3after 30 min of immersionare shown in

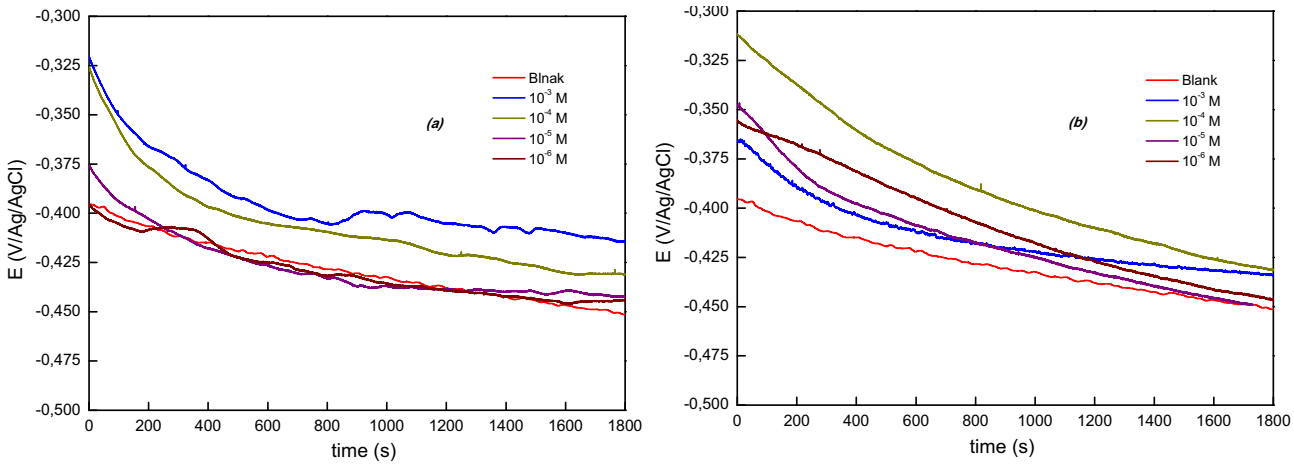

Fig. 4. Evolution of open circuit potential (OCP) versus time for mild steel in H_2SO_4 0.5 M with different concentrations of IM-Cl (a) and IM-CH_3 (b) at 298 K.

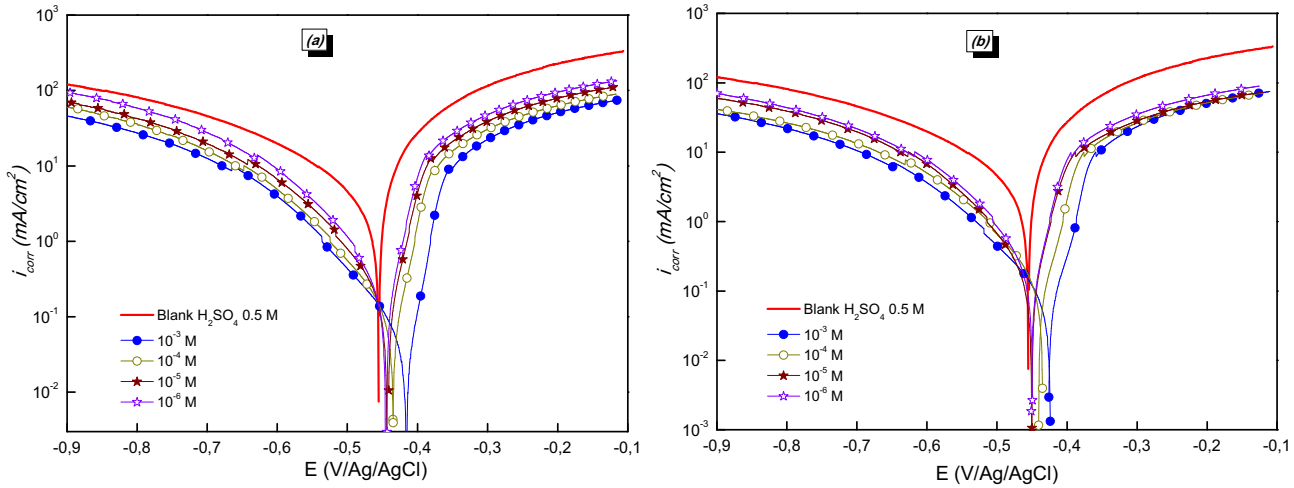

Fig. 5. Polarization curves for mild steel recorded in 0.5 M H_2SO_4 for selected concentrations of the inhibitors IM-Cl (a) and IM-CH_3 (b).

Table 4
Polarization parameters for mild steel in 0.5 M H_2SO_4in the absence and presence of different concentrations of IM-Cl and IM-CH_3.

Inhibitor	Conc. (M)	- E_{corr}vs Ag/AgCl (mV)	i_{corr} (μA/cm^2)	-βc mV/dec	βa mV/dec	IE%
Blank	–	451	1850	99	121	-
IM-Cl	10^{-6}	444	255	114	132	86,2
	10^{-5}	442	237	116	136	87,2
	10^{-4}	431	155	118	133	91,6
	10^{-3}	414	68,5	105	131	96,3
IM-CH_3	10^{-6}	446	320	99	125	82,7
	10^{-5}	449	270	94	132	85,4
	10^{-4}	433	263	95	137	85,8
	10^{-3}	422	154	106	133	91,7

Fig. 4. It was noticed that the addition of the inhibitors molecules induces shift in OCP (i.e., Ecorr).

3.3.2. *Polarization studies*

In order to know the kinetics of anodic and cathodic reactions, polarization experiments were carried out potentiodynamically in unagitated H_2SO_4 0.5 M solutions in the absence and presenceof different concentrations of inhibitors and the obtained polarization curves are shown in Fig. 5. The electrochemical parameters derived from Tafel curves are given in Table 4.

In acidic solutions, the anodic reaction is the movement of metal ions from the working electrode into thecorrosive solution, and the cathodic reaction is the discharge ofthe ions in the electrolyte such as the reduction of hydrogen ions to form hydrogen gas. The inhibitors may affect either the anodic, cathodic, or both reactions. Since the anodic Tafel slope (***βa***) and cathodic Tafel slope (***βc***) of imidazole were found to change with inhibitor concentration, the inhibitors affected both these reactions and referred to as mixed-type inhibitors. The adsorption of inhibitors can affect the corrosion rate in two ways:

- ✓ by decreasing the available reaction area, the so-called geometric blocking effect and
- ✓ by modifying the activation energy of the cathodic and/or anodic reactions occurring in the inhibitor-free metal in the course of the inhibited corrosion process.

It is a difficult task to determine which aspect of the inhibiting effect is connected to the geometric blocking action and which are connected to the energy effect. Theoretically, no shifts in E_{corr}should be observed after addition of the corrosion inhibitors if the geometric blocking effect is stronger than the energy effect [De Souza and Spinelli, 2009]. It is observed from Table 3 that the corrosion current density (i_{corr})decreases with increasing inhibitor concentration and it can be seen also that the corrosion potentials (E_{corr}) do not shift, which suggests that the both inhibitors act as very good organic inhibitors for mild steel in 0.5M

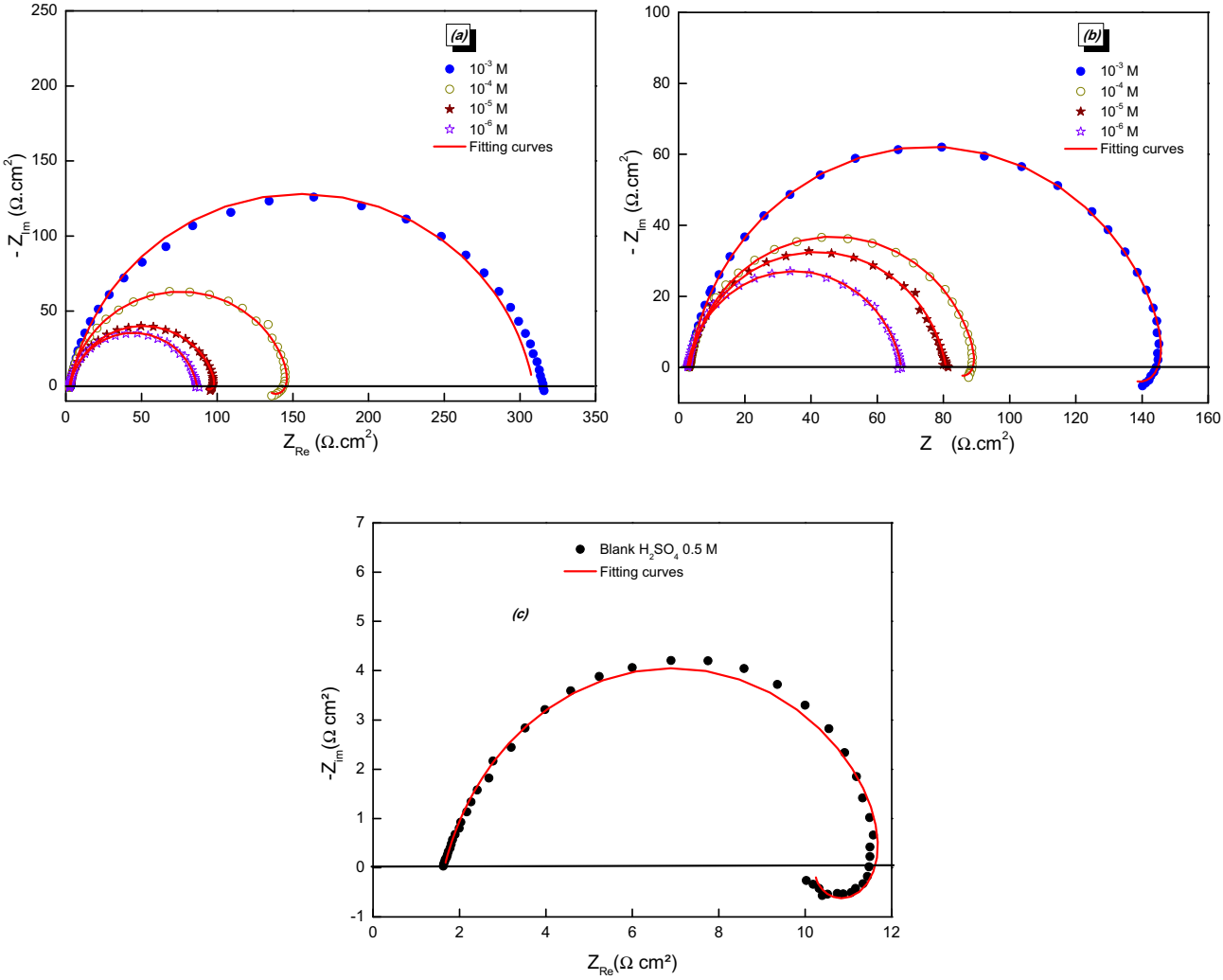

Fig. 6. Nyquist plots of mild steel in 0.5 M H_2SO_4 (c) solution in the absence and presenceof various concentrations of IM-Cl (a) and IM-CH_3 (b) at 298K.

H_2SO_4 solution.

The Tafel curves in solutions containing inhibitors do not shift, which suggests that the inhibitors could also suppress the anodic and cathodic reactions. An inhibitor can be classified as an anodic or cathodic type inhibitor when the displacement in E_{corr} value is >85 mV [Kowsari et al., 2014]. In the present study, it is found that the displacement exhibited by the studied inhibitors was <85 mV, which indicates that IM-Cl and IM-CH_3 act as mixed type inhibitors. Otherwise, the anodic and cathodic tafel slope values of inhibited solution have changed with respect to uninhibited solution, which also states that the tested inhibitors are of mixed type. The higher values of βa compared to those of βc at each concentration of the inhibitor further confirm that these inhibitors are regarded as mixed type inhibitors with anodic predominance. The obtained inhibition efficiencies values are in good agreement with those obtained bygravimetric measurements.

3.3.3. *EIS studies*

Electrochemical impedance spectroscopy (EIS) technique is popularly used in corrosion inhibitionto study the electrical properties of the metal/solutioninterface. The mechanistic information of the system under subject is provided by the nature and shape of the impedance curves [Asan et al., 2006]. This technique is extensively used in corrosion inhibition investigations. The electrochemical characteristics of mild steel in 0.5 M H_2SO_4 solution at 298 K in the absence and presenceof different concentrations of IM-Cl and IM-CH_3 (corrosion inhibitors) are presented as EIS Nyquist and Bode's plots in Figs. 6 and 7. In the Nyquist plot (Fig. 6) a depressed charge-transfer semicircle was appeared which is related to a single time constant shown in Bode's plot [El Mehdi et al., 2003; Wang et al., 2003]. But in blank solution and (10^{-4},10^{-5}) M of IM-Cl and (10^{-3},10^{-4}) M of IM-CH_3, we note a first loop at high frequency (*HF*) attributed to the relaxation of the double layer capacitance in parallel with the charge transfer resistance *Rt* inversely proportional to the corrosion rate and an inductive loop at low frequency (*LF*) [Lgaz et al., 2018a,b; Singh et al., 2009]. The LF inductive loop may be attributed to the relaxation process obtained by adsorption species as $SO_4^{2-}{}_{ads}$ and $H^+{}_{ads}$ on the electrode surface [Singh and Quraishi, 2010a, b]. It can be observed from Fig. 6 that the impedance response of IM-Cl and IM-CH_3has been considerably increased with increasing concentration of inhibitors to the electrolyte. The results obtained from EIS were of the similar orderas those obtained from polarization and gravimetric measurements.

The capacitive behavior of mild steel in the presence of IM-Cl and IM-CH_3could be visualized from Bode's plot (Fig. 7). A destructive outbreak of sulfuric acid corroded the mild steel and made the metal surface highly asymmetrical, which could be explained out bysmall phase angle. On the contrary, adsorption of the inhibitors on mild steel surface effectively lowered surface irregularities; additionally, we address the evolution of phase angle by measuring their values at arbitrarily chosen frequency (100 Hz) (Fig. 7). Clearly, with increasing concentration of both inhibitors the phase angle values dramatically increases as well.

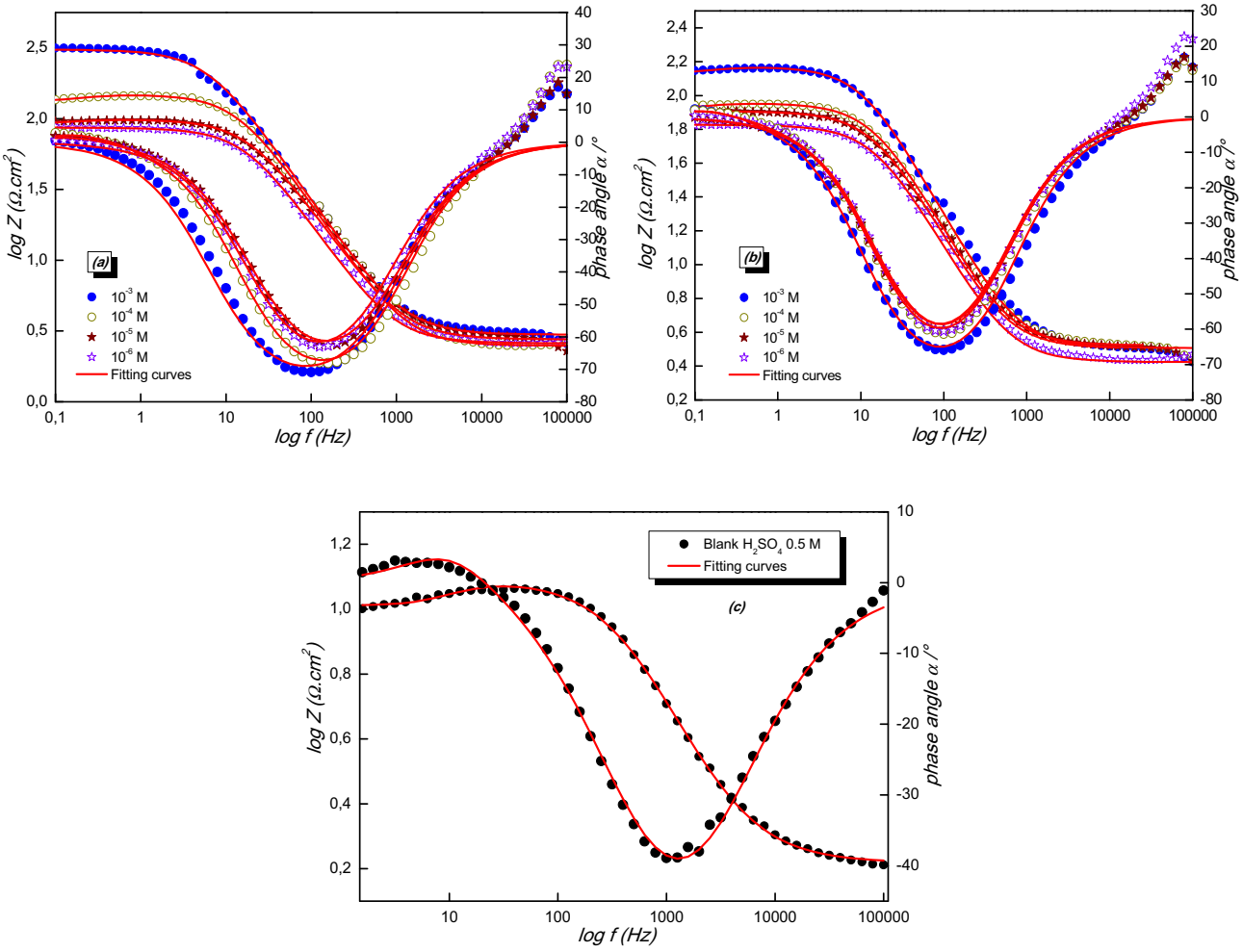

Fig. 7. Bode's plots and Phase angle values at 100 Hz at 298 K for mild steel in 0.5 M H_2SO_4 (c) solution in the absence and presence of various concentrations of IM-Cl (a) and IM-CH_3 (b).

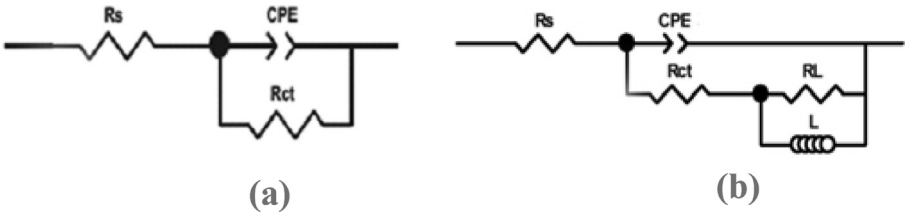

Fig. 8. The electrochemical equivalent circuit used to fit the impedance and bode's spectra/(a) charge-transfer semicircle, (b) charge-transfer semicircle and an inductive loop.

Furthermore, whatever the concentration used, the phase angle values are higher than that of the blank but lower than - 90° which also describes the non-ideal capacitor [Lgaz et al., 2018a,b]. This indicates anincreased capacitance of the interference due to the presence of

Table 5
Impedance parameters for mild steel in 0.5 M H_2SO_4 at 298 K in the absence and presence ofvarious concentrations of IM-Cl and IM-CH_3.

Inhibitor	Conc (M)	*Rs* (Ω.cm²)	*Q* ($\Omega^{-1}cm^2s^{-1}$)	*n*	C_{dl} (μF cm^{-2})	R_p (Ω.cm²)	R_L (Ω.cm²)	*L* (H)	χ^2	Θ	*EI%*
Blank	–	1.6 ± 0.2	430 ± 0.7	0.830 ± 0.003	180.0	11.7 ± 0.3	2.17 ± 0.1	0.48 ± 0.02	0.06	-	-
IM-Cl	10^{-6}	2.6 ± 0.3	179 ± 1.4	0.892 ± 0.005	108.0	83.98 ± 0.5	-	-	0.07	0.861	86,1
	10^{-5}	2.7 ± 0.3	149 ± 1.2	0.881 ± 0.01	83.77	89.62 ± 1.4	6.17 ± 0.18	6.96 ± 0.37	0.05	0.869	86,9
	10^{-4}	2.5 ± 0.2	117 ± 0.9	0.905 ± 0.01	75.92	130.9 ± 1.5	15.44 ± 0.2	11.24 ± 0.30	0.08	0.911	91,1
	10^{-3}	2.9 ± 0.2	124 ± 0.2	0.887 ± 0.005	82.14	306.0 ± 0.4	-	-	0.06	0.962	96,2
IM-CH_3	10^{-6}	2.6 ± 0.2	265 ± 2.3	0.887 ± 0.05	158.9	64.68 ± 0.5	-	-	0.07	0.819	81,9
	10^{-5}	3.2 ± 0.3	230 ± 1.8	0.888 ± 0.03	139.0	77.58 ± 0.4	-	-	0.08	0.849	84,9
	10^{-4}	3.3 ± 0.3	202 ± 1.9	0.894 ± 0.04	124.0	80.19 ± 1.5	6.93 ± 0.2	7.67 ± 0.4	0.09	0.854	85,4
	10^{-3}	3.2 ± 0.2	154 ± 1.5	0.901 ± 0.05	98.92	132.1 ± 1.4	13.17 ± 0.3	12.53 ± 0.33	0.1	0.911	91,1

adsorbed inhibitors molecules at the interface [Oguzie et al., 2007].

EIS and bode's spectra were analyzed using the equivalent circuits in Fig. 8.

The equivalent circuits used to model mild steel/solution interface for these systems are presented in Fig. 8.

The Table 5 results described below can be interpreted in terms of the equivalent circuitof the electrical double. The results show that the R_p values increases and C_{dl} decreases with increasing inhibitors concentration, which is attributed to the increase in surface coverage of mild steel by inhibitor molecules leadingto a decrease in the corrosion rate [El Ouali et al., 2010; Singh and Quraishi, 2010a,b]The decreased value of C_{dl} attributed towards decrease in local dielectric constant and/or an increase in the thickness of the protective layer, suggesting thatIM-Cl and IM-CH_3 act byadsorptionmechanism at mild steel/acid interface [Gerengi et al., 2012]. The capacitance of thedouble layer (C_{dl}) is linkedwith the thickness ofthe protective layer (d) by the following relation (6):

$$\text{Capacitance } C_{dl} = \frac{\varepsilon\varepsilon_0 S}{e} \tag{6}$$

Where $\mathcal{E}$ and $\mathcal{E}_o$ are dielectric constant of the medium and vacuum permittivity, e is the thickness of the protective layer and S is the surface area of the electrode.

With increase in the concentration of IM-Cl and IM-CH_3 the C_{dl} values are decreasing (Table 5) which depicts that the thickness of theprotective layer (e) is increasing. The values of n parameter are known as "phase shifts" which are often related to the degree of surface heterogeneity according to the following Eq. (7) [Ouakki et al., 2018a,b]:

$$C_{dl} = Q(\omega_{\max})^{\alpha-1} \tag{7}$$

Where, $\omega_{max} = 2\pi f_{max}$ is the angular frequency at the maximum value of the imaginary part of the impedance spectrum, Q is the admittance of the constant phase element (CFE) in Ω^{-1} cm^2 s^{-1}.

The values of the n parameter for inhibited systems are close to unity at higher concentrations implying thatthe interface behaves nearly capacitive [Singh et al., 2009; Quartarone et al., 2008]. The inhibition efficiencies of both products at 10^{-3} M reached 96.2% of IM-Cl and 91.1% of IM-CH_3, indicating that the synthesized compounds act as an effective corrosion inhibitors for mild steel in H_2SO_4 medium.

3.3.4. Adsorption isotherm and effect of temperature

3.3.4.1. Adsorption parameters. The interaction between the both inhibitor molecules and steel surface is best explained by adsorption isotherms. The efficiency of inhibitors is dependent mainly on their adsorption ability on the metal surface. The adsorption process involves replacement of water molecules at a metal solution interface [Gabrielli, 1980; Kalman et al., 1994; El-Taib Heakal et al., 2017] according to the following process:

$$Org_{(sol)} + nH_2O_{(ads)} \rightarrow Org_{(ads)} + nH_2O_{(sol)}$$

where $Org_{(sol)}$ and $Org_{(ads)}$ are the organic molecules in the solution and adsorbed on the metal surface, respectively, and n is the number of water molecules replaced by the organic molecules. In order to acquire more information regarding the interaction of these compounds and the surface of mild steel, it is important todetermine the mode of adsorption and the type of adsorption isotherm as there are ten different adsorption isotherms (Langmuir, Temkin, Freundlich, Frumkin, Modified, Langmuir, Henry, Viral, Damaskin, Volmer, and Flory–Huggins) [Oguzie et al., 2004; Bellman and Stamm, 2008; Mu et al., 2006] which were tested for their fit to the experimental data for the current investigation.

The best description of the adsorption behavior of studied inhibitorswas explained by Langmuir adsorption isotherm (Fig. 9) [Kalman et al., 1994], as the average linear regression coefficient values (R^2) obtained for IM-Cl and IM-$CH_3$and slope are very close to unity. All the

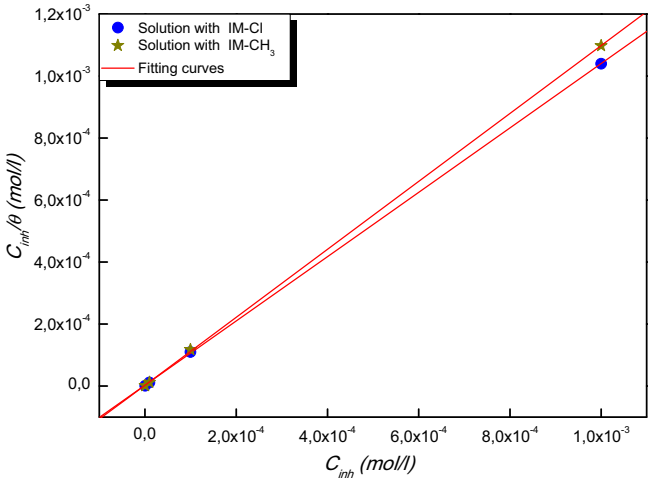

Fig. 9. Langmuir adsorption isotherm for mild steel in 0.5 M H_2SO_4 solution containing different concentrations of IM-Cl and IM-CH_3 at 298 K.

Table 6
Thermodynamic parameters for IM-Cl and IM-CH_3adsorption on mild steel surface in0.5M H_2SO_4 at 298 K.

Inhibitor	K_{ads} (L/mol)	ΔG_{ads} (Kj/mol)	R^2	Slope
IM-Cl	43.4 10^4	-42.11	0.99999	1.03755
IM-CH_3	37.4 10^4	-41.74	0.99998	1.09548

values are listed in Table 6. The isotherm is given by the following Eq. (8).

$$\frac{C_{inh}}{\theta} = \frac{1}{K_{ads}} + C_{inh} \tag{8}$$

where C_{inh} is the concentration of inhibitor, θ is the surface coverage degree, and K_{ads} is the adsorptive equilibrium constant. The linear relationships of C_{inh}/θ versus $C_{inh}$are depicted in Fig. 9.

The value of K_{ads} was found to be large, namely, 43.4 10^4 (L/mol)of IM-Cl and 37.4 10^4 (L/mol)of IM-CH_3, implying efficient adsorption and based on which the free energy of adsorption (ΔG_{ads}) was calculated using the following Eq. (9):

$$\Delta G_{ads} = -RT\ln(55.55 \times K_{ads}) \tag{9}$$

Where, R is universal gas constant and the absolute temperature is denoted by T. The molar concentration of water is expressed in mol/L and in solution its value is 55.5 [Flis and Zakroczymski, 1996].

Generally, values ofΔG_{ads} around or less than −20 kJ mol^{-1}suggested that the adsorption process is related with the electrostatic interaction between charged inhibitor molecules and the charged surface of the metal, which is termed as "physisorption" [Bellman and Stamm, 2008; Bentiss et al., 2005]; while values around or higher than −40 kJ mol^{-1} are associated with sharing of charge or transfer from the inhibitor molecules to the metal surface to form a coordinate type of metal bond termed as "chemisorption" [Mu et al., 2006; Eteram and Aisha, 2008].

In the present case of the adsorption of imidazole derivatives, ΔG_{ads} was determined to be -42.11 kJ/mol of IM-Cl and -41.74 kJ/mol of IM-CH_3, suggesting the chemical adsorption of the inhibitor molecules into the corroding metal surface.

3.3.4.2. Temperature kinetics. The influence of the reaction temperature on the potentiodynamic polarization curves in the absence and presence of 10^{-3} M of IM-Cl and IM-CH_3inhibitor's for mild steel in 0.5 M H_2SO_4 in the temperature range 298 ± 2 K to 328 ± 2 K are represented in Figs. 10 and 11.

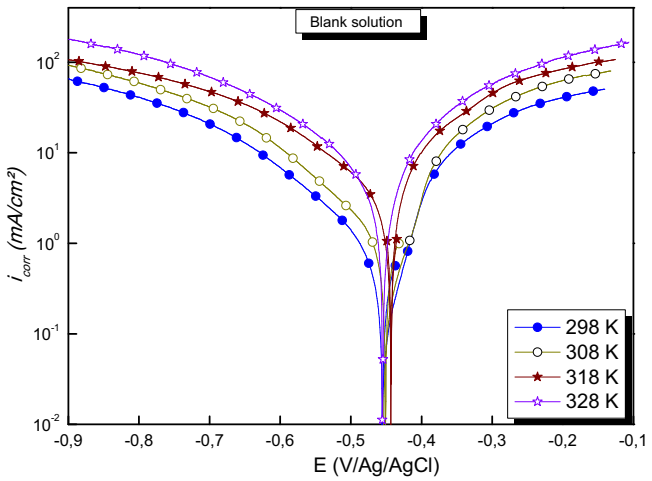

Fig. 10. Potentiodynamic polarization curves for mild steel immersedin 0.5 M H_2SO_4(Blank) at various temperatures between (298–328 ± 2 K).

There is a clear acceleration of both the cathodic and anodic reactions with an increase in temperature. As it is observed from the polarization parameters (Table 7), for mild steel, the corrosion current densities increased with the increase of temperature in 0.5 M H_2SO_4 solution in the absence and presence of 10^{-3} M of the studied inhibitors. These results could be attributed to the acceleration of chemical process as the temperature is increased such as electrochemical, chemical, transport [Nesic, 2007].

It is noted from Table 7 that, the inhibition efficiency reduced with temperature rise, indicating chemical adsorption of the imidazole molecules on the mild steel surface [Okafor et al., 2008].

3.3.5. Activation energy

The thermodynamic and kinetic parameters includingthe apparent activation energy (*Ea*), the enthalpy of activation (*ΔHa*) and the entropy of activation (*ΔSa*) for mild steel dissolution in 0.5 M H_2SO_4 solutions in the absence and presenceof 10^{-3}M of IM-Cl and IM-CH_3at 298–328 K were calculated from the Arrhenius Eq. (10) [Chetouani et al., 2005; Ekanem et al., 2010]:

$$i_{corr} = Ae^{-\frac{E_a}{RT}} \tag{10}$$

Taking the logarithm of both sides of the Arrhenius Eq. (11) could be obtained

$$\ln i_{corr} = \ln A - \frac{E_a}{RT} \tag{11}$$

The change of enthalpy {*ΔHa*} and entropy {*ΔSa*} for the formation of activated complex in the transition state was obtained from the transition state Eq. (12) [Singh and Quraishi, 2010a,b; Yadav et al., 2013].

$$\ln\left(\frac{i_{corr}}{T}\right) = \left[\ln\left(\frac{R}{hN_a}\right) + \left(\frac{\Delta S_a}{R}\right)\right] - \frac{\Delta H_a}{RT} \tag{12}$$

where i_{corr} is the corrosion current density, A is the pre-exponential factor, h is the Planck's constant, N_a is the Avogadro's number, *Ea* is the apparent activation energy, R is the gas constant (R = 8.314 J mol^{-1}. K^{-1}) and T is the absolute temperature.

A plot of ln (i_{corr}) vs 1000/T presented in Fig. 12a show straight line with slope of the line (-*Ea*/*R*). The values of *Ea* were calculated from the slope and given in Table 8. From the Table 8 it is clear that the *Ea* values of solution containing 10^{-3} M of IM-Cl and IM-CH_3 is higher than that in case of uninhibited solution which may be attributed to the formation of compact barrier film on the mild steel surface [Shaban et al., 2016]. The higher energy barrier for corrosion process in case of inhibited solutions suggest that adsorbed inhibitor's film prevents the charge/mass transfer reaction occurring on the surface [Murulana et al., 2016] and thus protecting metal from dissolution. The higher value of *Ea* for IM-Cl than that of IM-CH_3can be attributed to the fact that IM-Cl is substituted by the donor group corresponding to the mesomeric effect (Cl) whereas IM-CH_3 is substituted by an inductive effect group (CH_3).

A plot of ln (i_{corr}/T) vs 1000/T (Fig. 12b) gave a straight line with

Table 7
Polarization parameters for mild steel in 0.5 M H_2SO_4 with 10^{-3} M of IM-Cl and IM-CH_3at various temperatures.

Name of the inhibitor	Temperature K	- E_{corr} mV/Ag/AgCl	i_{corr} μA cm^{-2}	-β_c mV dec^{-1}	β_a mV dec^{-1}	η_{PP} %
Blank	298	451	1850	99	121	-
	308	453	2250	92	114	-
	318	449	2480	96	102	-
	328	442	3340	102	97	-
IM-Cl	298	414	68,5	105	131	96,3
	308	472	124	110	123	94.5
	318	477	196	107	124	92.1
	328	476	348	103	127	89.6
IM-CH_3	298	422	154	106	133	91,7
	308	484	227	105	135	89,9
	318	485	306	103	137	87,6
	328	482	484	99	140	85,5

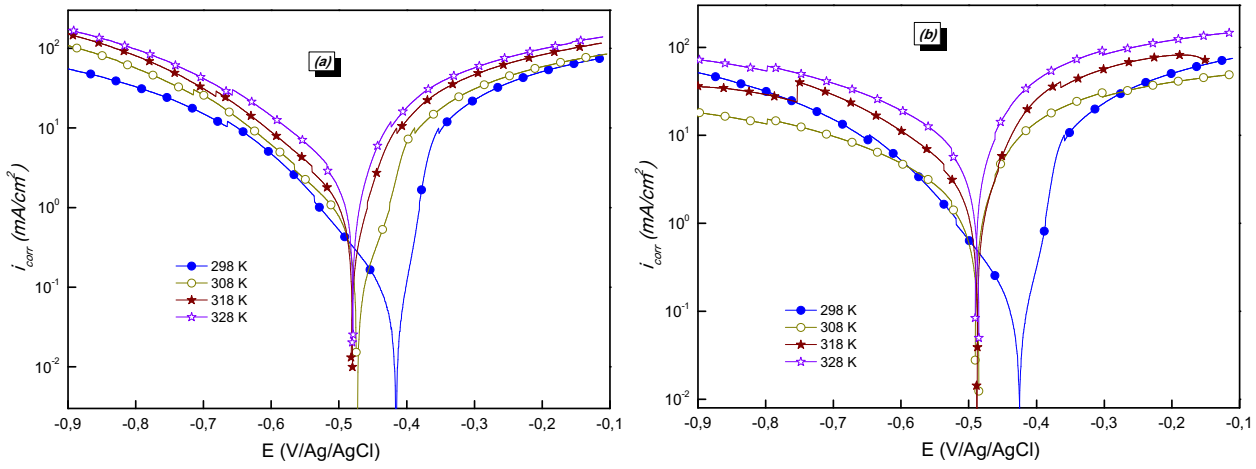

Fig. 11. Potentiodynamic polarization curves for mild steel immersed in 0.5 M H_2SO_4 in the present of 10^{-3} M of IM-Cl (a) and IM-CH_3 (b) at various temperatures between (298–328 ± 2 K).

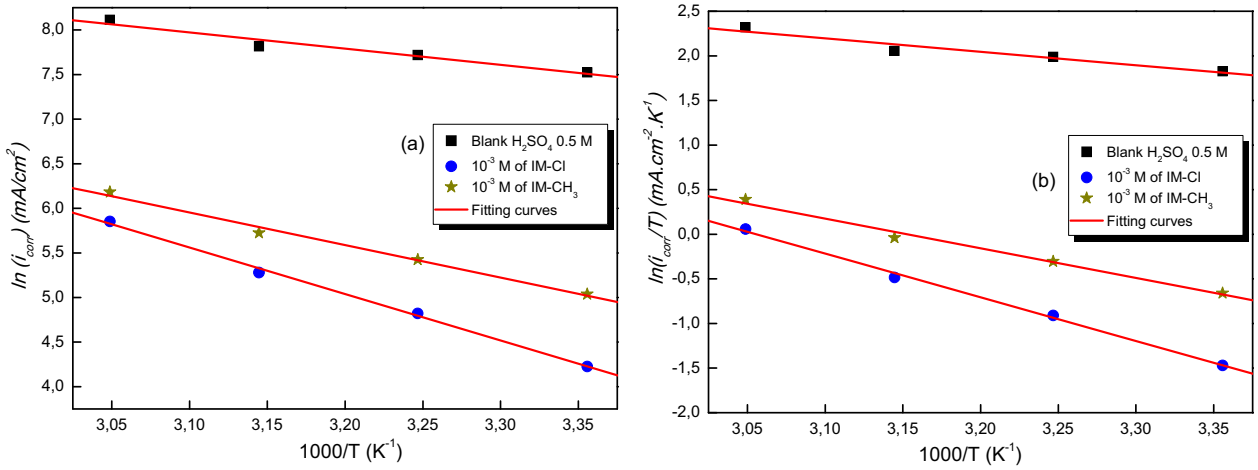

Fig. 12. Arrhenius plots for mild steel corrosion in 0.5 M H_2SO_4 in the absence and in presence of 10^{-3} M of IM-Cl and IM-CH_3/(a) of ln (i_{corr}) vs 1000/T and (b) ln (i_{corr}/T) vs 1000/T.

Table 8
Activation parameters for mild steel dissolution in 0.5 M Sulfuric acid solution in the absence and presence of optimum concentration of IM-Cl and IM-CH_3.

Medium	Concentration	Ea (KJ/mol)	ΔHa (KJ/mol)	ΔSa (KJ/mol.K)	Ea-ΔH
0.5 M H_2SO_4	Blank	15.00	12.50	-140.5	2.5
	10^{-3} M of IM-Cl	43.33	40.73	-70.0	2.6
	10^{-3} M of IM-CH_3	30.29	27.69	-110.2	2.6

slope of the line (-$\Delta Ha/R$) and an intercept (ln (R/hN_a) + ($\Delta Sa/R$) from which the values of ΔHa and ΔSa were calculated and summarized in Table 7. From these data, it was found that the thermodynamic parameters, ΔHa and $\Delta Sa$of dissolution reaction of mild steel in 0.5 M H_2SO_4 in the presence of 10^{-3} M of IM-Cl and IM-CH_3 were higher than uninhibited solution. The positive signs of the enthalpies ΔHareflected the endothermic nature of the steel dissolution process. The higher value of the entropy of activation, ΔSa in the presence of 10^{-3}M of IM-Cl and IM-CH_3 in solution compared to the case of the blank acid solution might be due to the enhanced randomness of the molecules [Martinez and Stern, 2002].

3.4. Surface analysis

In order to confirm the obtained results with electrochemical measurements. Qualitative microscopic analyses of MEB coupled with quantitative analyses EDX have been done. Fig. 13 shows MEB micrographs of the steel surface, before and after exposed in 0.5 M H_2SO_4 medium during 6 h at T = 298K, in absence and presence of both inhibitors. The characteristics of the parallel treatment on the polished surface of mild steel before immersion in the corrosive solution are

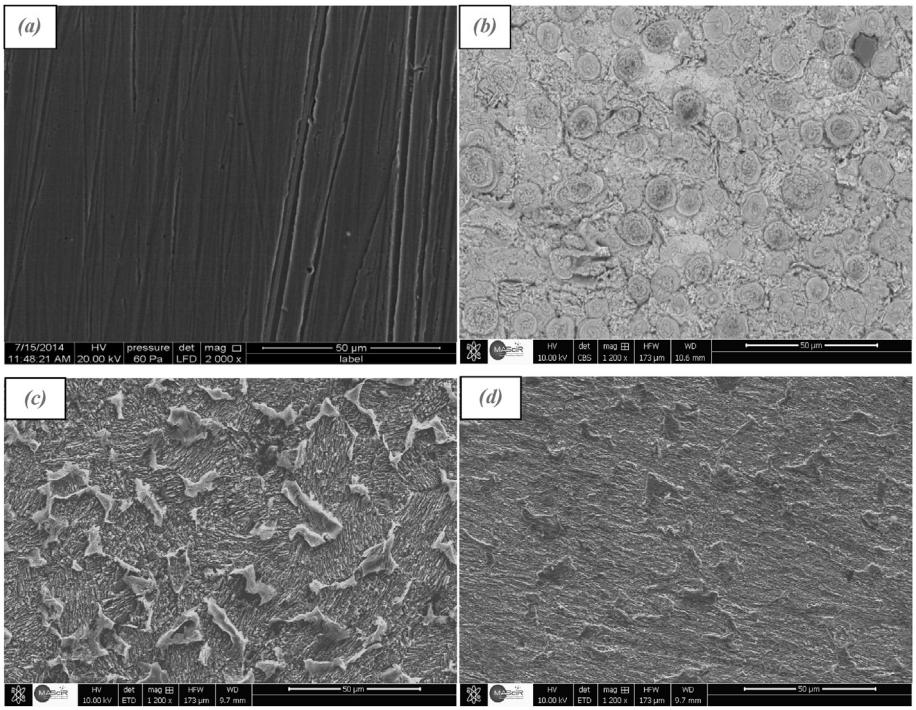

Fig. 13. SEM image (×50 μm) of mild steel before (a) and after 6 h of immersion in 0.5 M H_2SO_4 solution Blank (b) and solution with 10^{-3} M of inhibitors: IM-Cl (c) and IM-CH_3 (d) at 298 K.

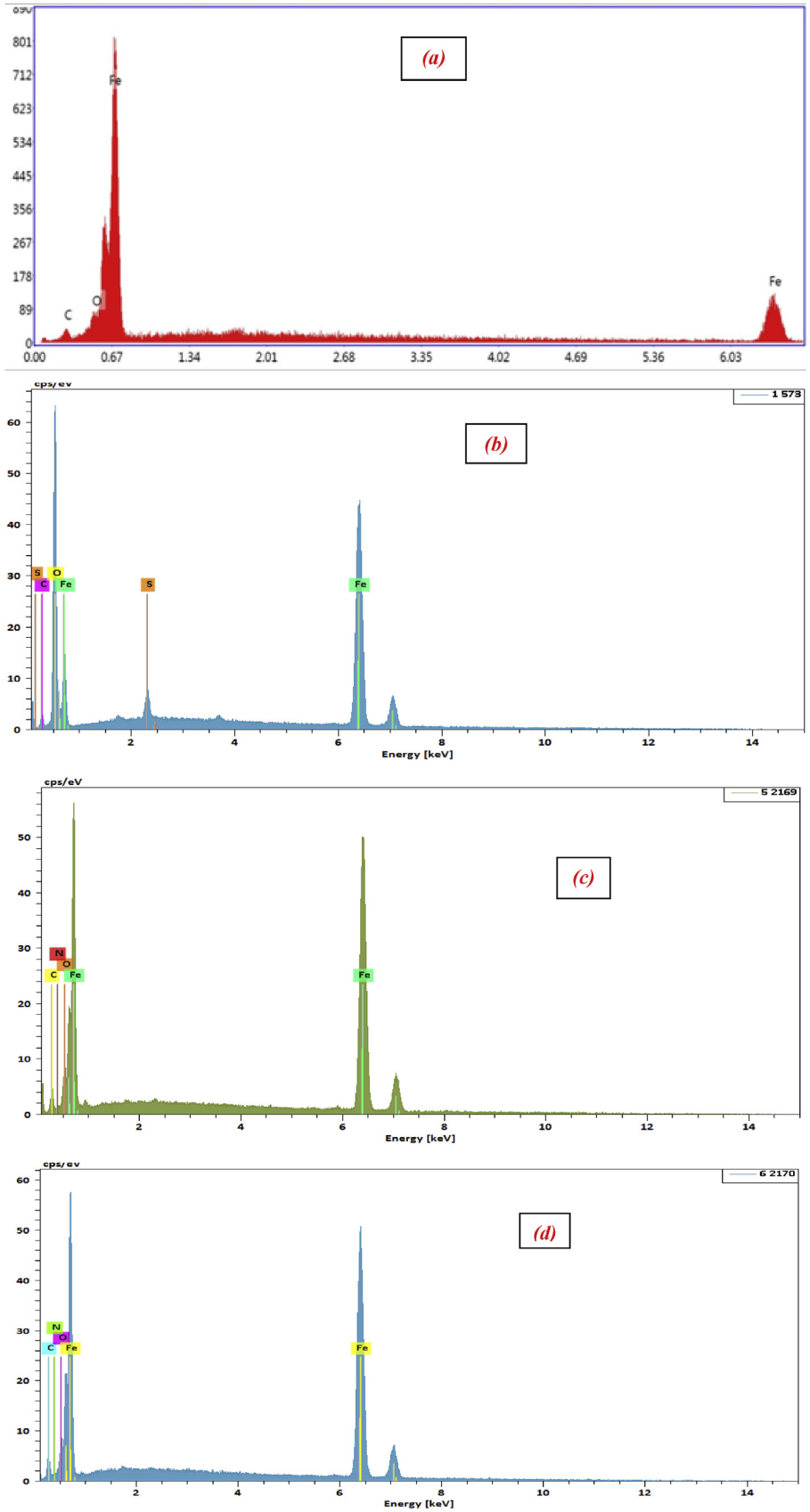

Fig. 14. Qualitative and quantitative EDAX analysis of the corroded surface before (a) and after 6h of immersion in the blank solution containing 0.5 M H_2SO_4 (b) and solution with 10^{-3} M of inhibitors: IM-Cl (c) and IM-CH_3 (d) at 298 K.

Table 9
%mass of the different elements resulting from the EDX analysis of the surface steel in 0.5 M H2SO4 in the absence and presenceof the inhibitors: IM-Cl and IM-CH_3 at 298 K.

Elements	% mass of steel only	% mass of steel in Blank solution	% mass of steel in blank solution with IM-Cl	% mass of steel in blank solution with IM-CH_3
C	4.6	3.95	3.26	4.56
O	4.4	19.22	2.79	2.78
N	–	–	0.29	0.38
S	–	1.70	–	–
Fe	91.0	72.4	95.26	92.94
Total	100.0	98.27	101.6	100.67

clearly visible in the image of mild steel only, which is associated with scratch friction.

The resulting of the high-resolution SEM micrograph shows that the steel surface was strongly damaged in the absence of the two inhibitors (Blank solution). However, there are less pits and cracks observed in the micrographs in the presence of IM-Cl and IM-CH_3 (Fig. 13) which suggests a formation of protective film on steel surface which was responsible for the corrosion inhibition [Ouakki et al., 2018a,b; Saxena et al., 2018; Tan et al., 2018]. Indeed, IM-Cl and IM-CH_3 has a strong tendency to adhere to the steel surface and can be regarded as good inhibitors for steel corrosion in 0.5 M H_2SO_4. The high inhibitive performance of these imidazole derivatives suggests a strong bonding of the IM-Cl and IM-CH_3on the metal surface due to presence of lone pairs from heteroatom (nitrogen) and π-orbitals, blocking the active sites and therefore decreasing the corrosion rate [Rbaa et al., 2019a,b].

EDX analyses (Fig. 14) shows a decrease in the peaks of O atoms and apparition of peaks of Nitrogen N, indicating that the molecules of the products IM-Cl and IM-CH_3 are strongly adsorbed on the metal surface and justifies the inhibitory role of this product (Table 9) [Suzuki et al., 1996; Shetty and Shetty, 2017; Rbaa et al., 2019a,b]. As a consequence, these results confirm those obtained with electrochemical measurements.

3.5. Quantum chemical calculations

Recently, Quantum chemical calculation using density function theory (DFT) was employed to explain and correlate the experimental results in order to give an overview ofthe inhibition action on the metal surface. The frontier orbital includingHOMO and LUMO of a chemical species are very important in defining its reactivity [Madkour and Elroby, 2015]. So, it becomes indispensable to investigate the electron distribution in HOMO and LUMO. The optimized structure and HOMO/LUMO distribution of neutral and protonated molecules are presented in Fig. 15. The HOMO and LUMO of IM-Cl and IM-CH_3 (neutral forms) are extended over the imidazole ring and the phenyl rings attached to the C1, C2 and C4 atoms. However, for the protonated forms the HOMO density is mostly distributed over the imidazole ring, Cl atom and the two phenyl rings areattached to C1 and C2 carbons. While, the LUMO density is delocalized with a high density on the imidazole ring and preferentially focused around the substituted phenyl rings for both inhibitors. The quantum chemical parameter for the inhibitors in neutral and protonated imidazole derivatives in gas phase and aqueous solution such as the energy of the highest occupied molecular orbital (HOMO), energy of the lowest unoccupied molecular orbital (LUMO), energy gap ($E_{gap} = E_{LUMO} - E_{HOMO}$), dipole moment ($\mu$), electronegativity ($\chi$), absolute hardness ($\eta$), absolute softness ($\sigma$) and fraction of transferred electrons (ΔN) were calculated and given in Table 10.

The value of E_{HOMO} is often associated with the electron donating ability of a molecule. High value of E_{HOMO} indicates the tendency of a molecule to donate electrons to an appropriate acceptor molecule with low energy and empty molecular orbital. However, the value of E_{LUMO}

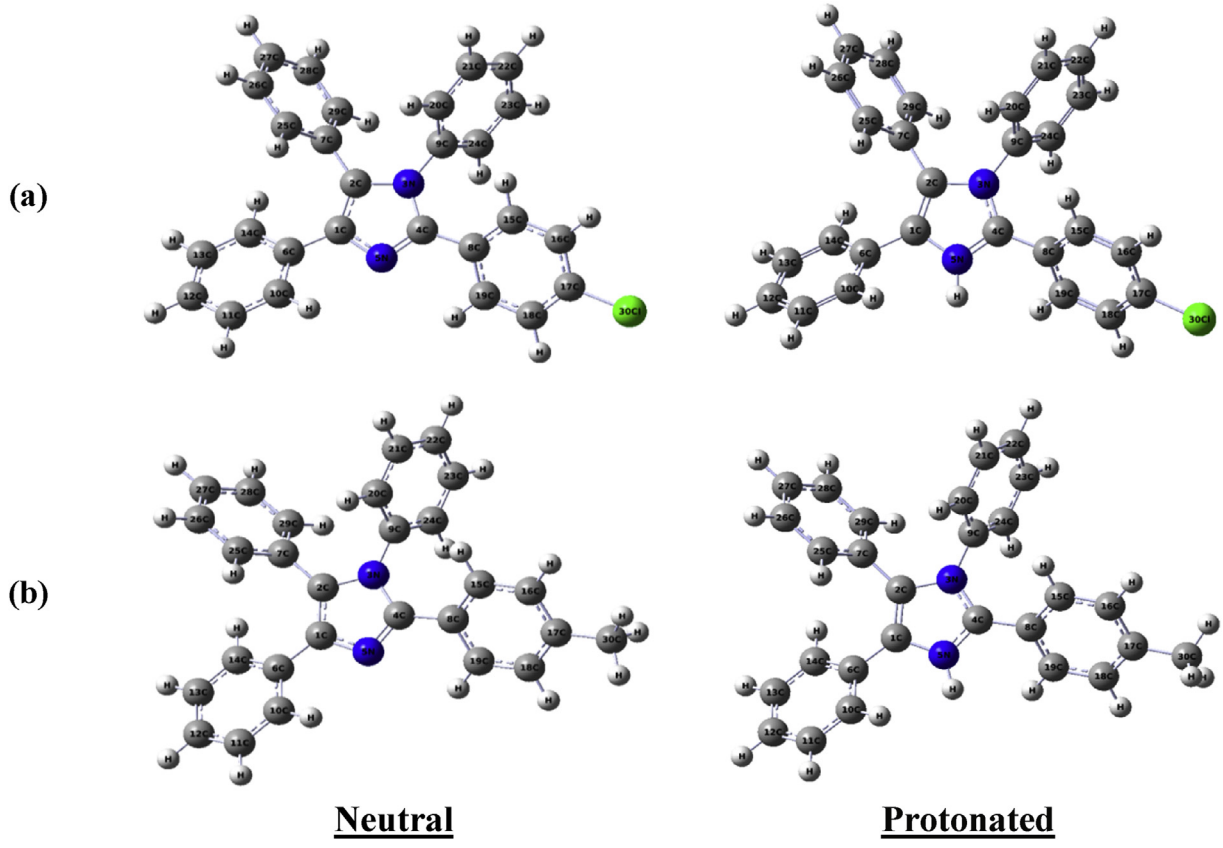

Fig. 15. Gas phase optimized structures of neutral and protonated forms of IM-Cl (a) and IM-CH_3 (b) at B3LYP/6-31G (d,p) level of theory.

Table 10
Calculated quantum chemical parameters for non-protonated and protonatedmolecules fIM-Cl and IM-CH_3obtained with the DFT at (B3LYP/6–31 (d,p) level in gas (G) and aqueous phases (A).

Parameter	Phase	IM-Cl	IM- CH_3	IM-Cl^+	(IM- CH_3)$^+$
E_{HOMO}(eV)	G	-5.3270	-5.1547	-8.3004	-8.9274
	A	-5.5417	-5.4581	-6.4617	-6.3814
E_{LUMO}(eV)	G	-1.0419	-0.8136	-4.1041	-4.5550
	A	-1.1146	-0.9159	-1.9842	-1.7842
ΔE_{gap} (eV)	G	4.2850	4.3411	4.1963	4.3724
	A	4.4271	4.5422	4.4774	4.5971
η(eV)	G	2.1425	2.1705	2.0981	2.1862
	A	2.2135	2.2711	2.2387	2.2985
σ(eV^{-1})	G	0.4667	0.4607	0.4766	0.4574
	A	0.4517	0.4403	0.4466	0.4350
χ(eV)	G	3.1844	2.9842	6.2022	6.7412
	A	3.3281	3.1870	4.2230	4.0828
ΔN	G	0.8904	0.9250	0.1900	0.0591
	A	0.8293	0.8394	0.6202	0.6345
μ(D)	G	4.83	4.1757	1.3143	2.4682
	A	6.4064	5.7676	1.9257	3.3976
Total energy	G	-43813.1627	-32376.6645	-43603.391	-32387.8875
	A	-43813.4550	-32376.9625	-43825.853	-32389.4391

shows the ability of a molecule to accept electrons [Madkour and Elroby, 2015; Khadiri et al., 2016]. The HOMO– LUMO gap, i.e., the difference in energy between the HOMO and LUMO is an important stability index. Smaller value of energy gap (ΔE) of the inhibitor molecules will render good inhibition efficiency, because the energy required to remove an electron from the lowest occupied orbital will be low [El Belghiti et al., 2016]. ΔN evaluates the electronic flow in a reaction of two systems with different electronegativities, in particular, an inhibitor molecule anda metallic surface. N values were calculated according to Pearson theory [El Belghiti et al., 2016] by the following Eq. (13):

$$\Delta N = \frac{\chi_{Fe} - \chi_{inh}}{2(\eta_{Fe} + \eta_{inh})} \tag{13}$$

While $\chi_{Fe} = 7$eVand $\eta_{Fe} = 0$ eV are the theoretical values of electronegativity and hardness for iron.

It was pointed out that the positive number of electrons transferred (ΔN) indicates that the molecule act as an electron acceptor, while a negative number of electrons transferred (ΔN) indicates that the molecule act as electron donor [Erdogan et al., 2017]. Both of the ΔN values are positive, which demonstrates thatIM-Cl and IM-CH_3can donate electrons to the iron surface to form self-assembled layers of inhibitors.

In terms of reactivity, soft molecules are more reactive than hard ones since they have small energy gap that can enable the easy transfer of electrons [Elemike Elias et al., 2017]. The hardness value of a molecule can be determined by the formula (14) [Mahalakshmi and Balachandran, 2015]:

$$\eta = \frac{(E_{LUMO} - E_{HOMO})}{2} \tag{14}$$

Where, E_{HOMO} and E_{LUMO} are the energies of the HOMO and LUMO orbitals.

IM-Cl with the largest inhibition efficiency has the smallest hardness value 2.1425 eV. Additionally, IM-Cl has the largest softness (the inverse of hardness), $\sigma = 0.4667$. The dipole moment (μ) is another important electronic parameter that results from a non-uniform distribution of charges on the various atoms in the molecule. The high value of the dipole moment most likely increases the adsorption of the inhibitor on the metal surface [Wazzan, 2014]. It is clear that increasing values of E_{HOMO}, softness and ΔN follows the trend IM-Cl > IM-CH_3 and the decreasing values of E_{LUMO}, hardness and the energy gap follows the order IM-Cl < IM-CH_3indicating that the inhibition efficiency of IM-Cl is better than that of IM-CH_3. The substitution of the methyl group in IM-CH_3 by the Cl atom results in an increase in the density of the entire molecule (IM-Cl) and facilitates their adsorption onto steel surface. This is in good agreement with the experimental results which showed that IM-Cl has higher efficiency than IM-CH_3. As we know that the values of ΔE_{gap} in the both inhibitors are lower in neutral forms than protonated forms, which reveal that neutral species can easily adsorb on the steel surface than protonated forms.

The different values of the electrostatic potential at the surface are represented by different colors. Potential increases in the order red < orange < yellow < green < blue. The negative electrostatic potentials are shown in red region, the intensity of which is proportional to the absolute value of the potential energy, and positive electrostatic potentials are shown in blue region [Mahalakshmi and Balachandran, 2015]. The total electron density surfaceismapped with the electrostatic potential (ESP) and the electrostatic potential contour maps. It is obviously from the Fig. 16 that the region around imidazole ring and chlorine atoms represents the most negative potential region (red to yellow), while more positive charge around the ring hydrogen atoms. The molecular electrostatic potentials (ESP) and ESP contours of thestudied imidazole derivatives are presented in Fig. 17.

The adsorption of the inhibitor molecule on the metal surface takes place by the donor-acceptor interaction, which can be analyzed by the local reactivity i.e. condensed Fukui functions at DFT-B3LYP/6-31G (d,p) level of theory. These descriptors are measurements of the chemical reactivity, as well as an indicative of the nucleophilic and electrophilic behavior of the inhibitor molecule. The condensed Fukui functions calculated by natural population analysis (NPA)using the following Eqs. (15) and (16) [Khaled, 2010]:

$$\text{For nucleophilic attack: } f_k^+ = q_k(N+1) - q_k(N) \tag{15}$$

$$\text{For electrophilic attack: } f_k^- = q_k(N) - q_k(N-1) \tag{16}$$

where q_k is the gross charge of atom k in the molecule and N is the number of electrons.

Fukui indices from the calculations for the charged species (N+1 and N–1) as well as the neutrals molecules in the both phases are given in Table 11, respectively. For simplicity, only the charges and Fukui functions over the heteroatoms and some carbons of inhibitors the most reactive are presented. The maximum value of f_k^+ index is related to reactivity pertaining to a nucleophilic attack whereas the maximum of f_k^- index indicates the favored site for adsorption of electrophilic agents [Singh et al., 2017]. The higher value of f_k^- suggests acceptance of electron from the metal and higher value of f_k^+ suggests higher electron donation ability of inhibitor molecules [Masroor et al., 2017]. In the case of IM-Cl, the largest values of f_k^- are located on Cl30, C2 and C4 atoms which indicates that these atoms prefer to form a chemical bond by

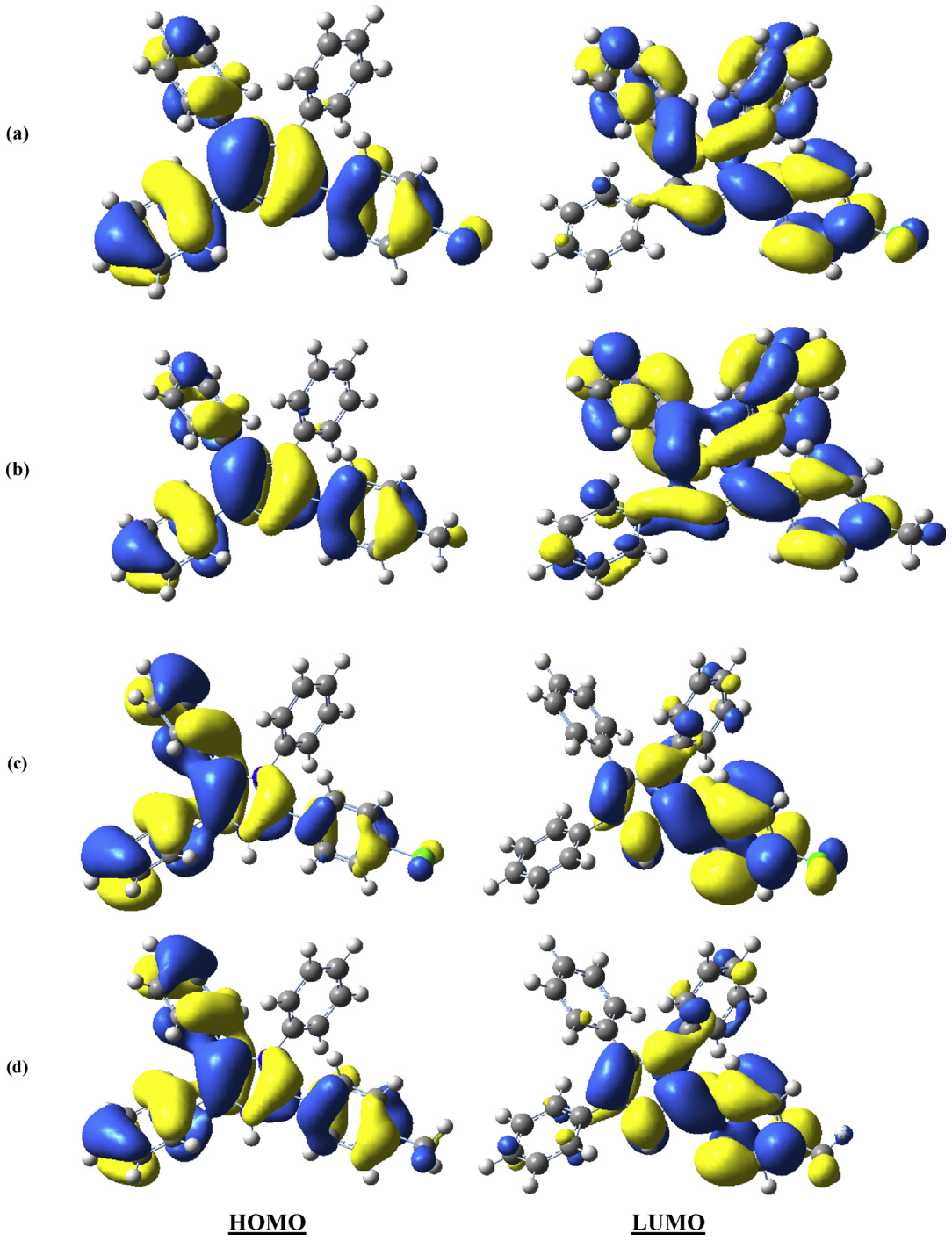

Fig. 16. HOMO and LUMO surfaces of the neutral and protonated forms of imidazole compounds in gas phase using DFT/6-31G (d,p) calculation level: IM-Cl (a), IM-CH_3 (b), IM-Cl^+ (c) and IM-CH_3^+ (d).

donation of electrons to the metal surfaceand the favorable sites for electron acceptance (f_k^+) i.e., nucleophilic attacks are Cl30, C2, C4, C1 and C12 atoms. In IM-CH_3case, the favorable sites for electrophilic attacks are C4, C2 and N5 atoms while the favorable sites for nucleophilic attacks are C2, C4, C1 and N5 atoms. After the analysis, it can be concluded that the C4, C2 and N5 atoms of the imidazole ring are more responsible for donor-acceptor interactions and thus facilitate the adsorption of the both inhibitors over the metallic surface. It is also possible to observe from Table 11 that the Cl30 atom in IM-Cl is the most susceptible site for electrophilic and nucleophilic attack in the gas and aqueous phases, indicating that IM-Cl has the highest reactivity in comparison to IM-Cl and would therefore likely interact strongly with the metal surface.

3.6. Molecular dynamic simulations

The interaction of compounds with metal surface at the atomic level is widely investigated by Molecular dynamics simulations [Khadiri et al., 2018]. This theoretical method holds a great promise to mimic the real corrosion environment and explore themolecular processes related to the corrosion behavior of metal in aqueous solutions and inhibition mechanism [Lgaz et al., 2018a,b]. In this section, we aim to obtain insightful

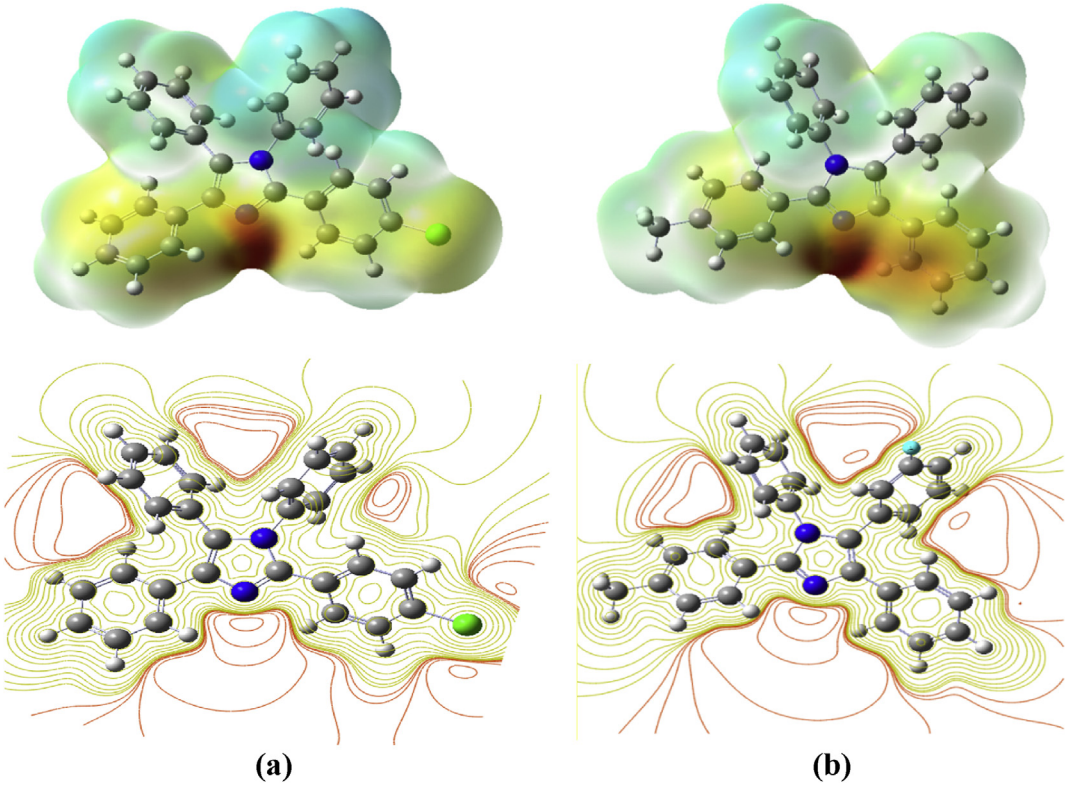

Fig. 17. ESP maps and contours of mentioned inhibitors at B3LYP/6–31 (d,p) level: IM-Cl (a) and IM-CH_3 (b).

Table 11
Calculated Fukui functions of IM-$CH_3$and IM-Cl calculated at B3LYP/6-31G (d,p) in gas (G) and aqueous (A) phases.

Inhibitor	Atom k	phase	P(N)	P(N+1)	P(N-1)	f_k^+	f_k^-
IM-Cl	30Cl	G	-0.0127	0.0756	-0.0924	0.0883	0.0797
		A	-0.0251	0.0245	-0.0946	0.0497	0.0694
	2C	G	0.1971	0.2798	0.1680	0.0827	0.0290
		A	0.2119	0.3210	0.1603	0.1091	0.0515
	4C	G	0.3944	0.4542	0.3627	0.0598	0.0316
		A	0.2119	0.3210	0.1603	0.1091	0.0515
	N5	G	-0.5556	-0.5324	-0.5801	0.0231	0.0245
		A	-0.5858	-0.5585	-0.6160	0.0272	0.0302
	12C	G	-0.0824	-0.0590	-0.0908	0.0233	0.0084
		A	-0.0993	-0.0684	-0.1062	0.0309	0.0068
IM-CH_3	C2	G	0.1895	0.2705	0.1650	0.0809	0.0245
		A	0.2051	0.3091	0.1552	0.1039	0.0498
	C4	G	0.3929	0.4476	0.3651	0.0547	0.0277
		A	0.3971	0.4785	0.3459	0.0813	0.0512
	O30	G	-0.5344	-0.5008	-0.5455	0.0336	0.0110
		A	-0.5480	-0.5200	-0.5565	0.0280	0.0085
	C1	G	0.1600	0.1910	0.1438	0.0309	0.0161
		A	0.1457	0.2003	0.1260	0.0545	0.0197
	N5	G	-0.5633	-0.5385	-0.5858	0.0247	0.0225
		A	-0.5951	-0.5649	-0.6159	0.0302	0.0208

explanation of the fundamental inhibition processes that determine the action of inhibitors as corrosion inhibitors [El Bakri et al., 2018]. In Fig. 18, the side view of molecular interaction of inhibitor on C-steel surface after reaching equilibrium is presented in the presence of simulated acid solution of 0.5 M H_2SO_4. It can be seen that the inhibitors in the final configuration of the simulation system was close to the Fe surface. Interestingly, the IM-Cl inhibitor molecule is oriented more parallel to the Fe surface than IM-CH_3. Meaning thatmore surface coverage is achieved by IM-Cl inhibitor than IM-CH_3; hence IM-Cl is expected to give higher inhibition than IM-CH_3. The adsorption energies of inhibitor molecules obtained under equilibrium conditions are -227.75 kcal/mol and -245.73 kcal/mol for IM-CH_3 and IM-Cl, respectively. It is also clear that the adsorption of $SO_4^{2-}$is around -600 Kcal/mol which aretwice more than the adsorption of inhibitors; this means that SO_4^{2-} ions have higher affinity to metal surface and the adsorption of compounds on metal surface proceeds physically via competing adsorption and interaction between inhibitors and sulfate ions adsorbed on Fe surface. Moreover the presence of Cl atom in IM-Cl stabilizes the charges on the aromatic moieties and facilitates the adsorption of compounds on metal surface.

4. Conclusion

The following conclusions can be derived from the study of Corrosion inhibition characteristics of two organic compounds of imidazole

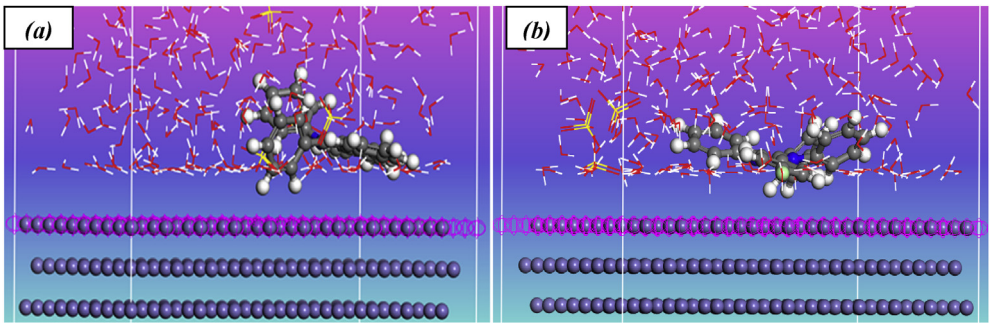

Fig. 18. Most stable orientation of inhibitors on Fe (110) surface in 0.5 M H_2SO_4/IM-CH_3 (a) and IM-Cl (b).

derivatives, IM-Cl and IM-CH_3on mild steel corrosion in 0.5 M H_2SO_4 medium:

- Both IM-Cl and IM-CH_3 are efficient corrosion inhibitors for mild steel in the studied medium.
- Polarization measurements showed that both IM-Cl and IM-CH_3 are mixed type inhibitors.
- The results of EIS indicate that the values of C_{dl}tend to decrease and both *Rct* and $\eta\%$ tends to increase with increasing the inhibitors concentrations. These results can be attributedto an increase of the thickness of the protective film formed on the mild steel surface.
- The adsorption characteristics of both IM-Cl and IM-CH_3followed the Langmuir adsorption isotherm model.
- From the obtained values of kinetic and thermodynamic parameters (Ea, ΔG_{ads}) our imidazole derived acts as chemisorption and physisorption mechanism.
- Reasonably good agreement was observed between the obtained measures from weight loss, potentiodynamic polarization curves and electrochemical impedance spectroscopy techniques.
- The study of morphology of the surface steel by MEB coupled with the EDX shows the existence of a stable and insoluble adherent deposit which limits the access of the electrolyte to the surface of the metal
- TheIM-Cl compound has the highest reactivity in comparison to IM-$CH_3$and would therefore likely interact strongly with the metal surface.
- Good agreement between thetheoretical and experimental resultswas obtained.

Declarations

Author contribution statement

M. Ouakki: Conceived and designed the experiments; Performed the experiments; Wrote the paper.

M. Galai, B. Lakhrissi: Analyzed and interpreted the data; Wrote the paper.

M. Rbaa, E. H. Rifi: Performed the experiments; Analyzed and interpreted the data.

A.S. Abousalem: Performed the experiments; Contributed reagents, materials, analysis tools or data.

M. Cherkaoui: Conceived and designed the experiments; Analyzed and interpreted the data; Wrote the paper.

Funding statement

This research did not receive any specific grant from funding agencies in the public, commercial, or not-for-profit sectors.

Competing interest statement

The authors declare no conflict of interest.

Additional information

No additional information is available for this paper.

References

Abdullah Dar, M., 2011. A review: plant extracts and oils as corrosion inhibitors in aggressive media. Ind. Lubr. Tribol. 63, 227.

Alaoui, K., Touir, R., Galai, M., Serrar, H., Ouakki, M., Kaya, S., Tüzün, B., Boukhris, S., Ebn Touhami, M., El Kacimi, Y., 2018. Electrochemical and computational studies of some triazepine carboxylate compounds as acid corrosion inhibitors for mild steel. J. Bio- and Tribo-Corros. 4, 37.

Amin, M.A., Abd-El-Rehim, S.S., El-Sherbini, E.E.F., Hazzazi, O.A., 2009. Polyacrylic acid as a corrosion inhibitor for Al in weakly alkaline solutions. Corros. Sci. 51, 658–667.

Aouniti, A., Hammouti, B., Kertit, S., Brighli, M., 1998. The inhibitive effect of some pyridines towards the corrosion of iron in hydrochloric acid solution. Bull. Electrochem. 14, 193.

Asan, A., Soylu, S., Kıyak, T., Yıldırım, F., Oztas, S.G., Ancın, N., Kabasakaloğlu, M., 2006. Investigation on some Schiff bases as corrosion inhibitors for mild steel. Corros. Sci. 48, 3933.

Becke, A.D., 1993. Density functional thermochemi-stry. III. The role of exact exchange. J. Chem. Phys. 98, 5648–5652.

Bedair, M.A., El-Sabbah, M.M.B., Fouda, A.S., Elaryian, H.M., 2017. Synthesis, electrochemical and quantum chemical studies of some prepared surfactants based on azodye and Schiff base as corrosion inhibitors for steel in acid medium. Corros. Sci. 128, 54–72.

Bellman, C., Stamm, M., 2008. Polymer Surfaces and Interfaces. Springer, Berlin.

Bentiss, F., Traisnel, M., Gengembre, L., Lagrene'e, M., 1999. A new triazole derivative as inhibitor of the acid corrosion of mild steel: electrochemical studies, weight loss determination, SEM and XPS. Appl. Surf. Sci. 152, 237.

Bentiss, F., Lebrini, M., Lagrenee, M., 2005. Thermodynamic characterization of metal dissolution and inhibitor adsorption processes in mild steel/2, 5-bis (n-thienyl)-1, 3, 4-thiadiazoles/hydrochloric acid system. Corros. Sci. 47, 2915.

Chetouani, A., Hammouti, B., Benhadda, T., Daoudi, M., 2005. Inhibitive action of bipyrazolic type organic compounds towards corrosion of pure iron in acidic media. Appl. Surf. Sci. 249, 375.

De Souza, F.S., Spinelli, A., 2009. Caffeic acid as a green corrosion inhibitor for mild steel. Corros. Sci. 51, 642–649.

Ech-chihbi, E., Salim, R., Oudda, H., Elaatiaoui, A., Rais, Z., Oussaid, A., El Hajjaji, F., Hammouti, B., Elmsellem, H., Taleb, M., 2016. Effect of some imidazopyridine compounds on carbon steel corrosion in hydrochloric acid solution. Der Pharma Chem. 8 (13), 214–230.

Ech-chihbi, E., Belghiti, M.E., Salim, R., Oudda, H., Taleb, M., Benchat, N., Hammouti, B., El-Hajjaji, F., 2017. Experimental and computational studies on the inhibition performance of the organic compound "2-phenylimidazo [1, 2-a] pyrimidine-3-carbaldehyde" against the corrosion of carbon steel in 1.0 M HCl solution. J. Surf. Interface. 9, 206–217.

Ekanem, U.F., Umoren, S.A., Udousoro, I.I., Udoh, A.P., 2010. Inhibition of mild steel corrosion in HCl using pineapple leaves (Ananas comosus L.) extract. J. Matter. Sci. 45, 5558–5566.

El Bakri, Y., Guo, L., Harmaoui, A., Ali, A.B., Essassi, E.M., Mague, J.T., 2018. Synthesis, crystal structure, DFT, molecular dynamics simulation and evaluation of the anticorrosion performance of a new pyrazolotriazole derivative. J. Mol. Struct.

El Belghiti, M., Karzazi, Y., Dafali, A., Hammouti, B., Bentiss, F., ObotI, B., Bahadur, I., Ebenso, E.E., 2016. Experimental, quantum chemical and Monte Carlo simulation studies of 3,5-disubstituted-4-amino-1,2,4-triazoles as corrosion inhibitors on mild steel in acidic medium. J. Mol. Liq. 218, 281–293.

El Faydy, Mohamed, Galai, Mouhsine, Rbaa, Mohamed, Ouakki, Moussa, Lakhrissi, Brahim, Touhami, Mohamed Ebn, El Kacimi, Younes, 2018. Synthesis and application of new quinoline as hydrochloric acid corrosion inhibitor of carbon steel. Anal. Bioanal. Electrochem. 10 (7), 815–839.

El Mehdi, B., Mernari, B., Traisnel, M., Bentiss, F., Lagrenee, M., 2003. Synthesis and comparative study of the inhibitive effect of some new triazole derivatives towards corrosion of mild steel in hydrochloric acid solution. Mater. Chem. Phys. 77, 489.

El Ouali, I., Hammouti, B., Aouniti, A., Ramli, Y., Azougagh, M., Essassi, E.M., Bouachrine, M., 2010. Thermodynamic characterisation of steel corrosion in HCl in the presence of 2- phenylthieno (3, 2-b) quinoxaline. J. Mater. Environ. Sci. 1, 1.
El-Ouafi, A., Hammouti, B., Oudda, H., Kertit, S., Touzani, R., Ramdani, A., 2002. New bipyrazole derivatives as effective inhibitors for the corrosion of mild steel in 1M HCl medium. Anti-Corros. Meth. Mater. 49, 199.
El-Taib Heakal, F., Deyab, M.A., Osman, M.M., Nessim, M.I., Elkholy, A.E., 2017. Synthesis and assessment of new cationic gemini surfactants as inhibitors for carbon steel corrosion in oilfield water. RSC Adv. 47335–47352.
Elemike Elias, E., Nwankwo Henry, U., Onwudiwe Damian, C., Hosten Eric, C., 2017. Synthesis, crystal structures, quantum chemical studies and corrosion inhibition potentials of 4-(((4 ethylphenyl)imino)methyl)phenol and (E)-4-((naphthalen-2-ylimino) methyl) phenol Schiff bases. J. Mol. Struct. 1147, 252–265.
Erdogan, Saban, Safi, Zaki S., Kaya, Savas, Isın, Dilara Ozbakır, Guo, Lei, Kaya, Cemal, 2017. A computational study on corrosion inhibition performances of novelquinoline derivatives against the corrosion of iron. J. Mol. Struct. 1134, 751–761.
Eteram, A.N., Aisha, A.H., 2008. Thermodynamic study of metal corrosion and inhibitor adsorption processes in mild steel/1-methyl-4 [40 (-X)-styryl pyridinium iodides/ hydrochloric acid systems. Mater. Chem. Phys. 110, 145.
Flis, J., Zakroczymski, T., 1996. Impedance study of reinforcing steel in simulated pore solution with tannin. J. Electrochem. Soc. 143, 2458.
Fouda, A.S., Ismail, M.A., EL-ewady, G.Y., Abousalem, A.S., 2017a. Evaluation of 4-amidinophenyl-2, 2′-bithiophene and its aza-analogue as novel corrosion inhibitors for CS in acidic media: experimental and theoretical study. J. Mol. Liq. 240, 372–388.
Fouda, A.S., Ismail, M.A., Abousalem, A.S., Elewady, G.Y., 2017b. Experimental and theoretical studies on corrosion inhibition of 4-amidinophenyl-2, 2′-bifuran and its analogues in acidic media. RSC Adv. 7 (73), 46414–46430.
Gabrielli, C., 1980. Identification of Electrochemical Processes by Frequency Response Analysis. Solartron, Franborough, UK, p. 62.
Galai, M., Rbaa, M., El Kacimi, Y., Ouakki, M., Dkhirech, N., Touir, R., Lakhrissi, B., EbnTouhami, M., 2016. Anti-corrosion properties of some triphenylimidazole substituted compounds in corrosion inhibition of carbon steel in 1. 0 M hydrochloric acid solution. Anal. Bioanal. Electrochem. 9, 80.
Galai, M., El Faydy, M., El Kacimi, Y., Dahmani, K., Alaoui, K., Touir, R., Lakhrissi, B., Ebn Touhami, M., 2017. Synthesis, characterization and anti-corrosion properties of novel quinolinol on C-steel in a molar hydrochloric acid solution. Port. Electrochim. Acta 35, 233.
Gasiorek, J., Szczurek, A., Babiarczuk, B., Kaleta, J., Jonesn, W., Krzak, J., 2018. Functionalizable sol-gel silica coatings for corrosion mitigation. Materials 11, 197.
Gerengi, H., Sahin, H.I., 2012. Schinopsis lorentzii extract as a green corrosion inhibitor for low carbon steel in 1 M HCl solution. Ind. Eng. Chem. Res. 51, 780.
Gupta, N.K., Quraishi, M.A., Verma, C., Mukherjee, A.K., 2016a. Green Schiff's bases as corrosion inhibitors for mild steel in 1 M HCl solution: experimental and theoretical approach. RSC Adv. 6, 102076–102087.
Gupta, N.K., Quraishi, M.A., Verma, C., Mukherjee, A.K., 2016b. Schiff's bases derived from l-lysine and aromatic aldehydes as green corrosion inhibitors for mild steel: experimental and theoretical studies. J. Mol. Liq. 215, 47–57.
Hammouti, B., Aouniti, A., Taleb, M., Brighli, M., Kertit, S., 1995. L-methionine methyl ester hydrochloride as a corrosion inhibitor of iron in acid chloride solution. Corrosion 51, 411.
Haque, J., Ansari, K.R., Srivastava, V., Quraishi, M.A., Obot, I.B., 2017. Pyrimidine derivatives as novel acidizing corrosion inhibitors for N80 steel useful for petroleum industry: a combined experimental and theoretical approach. J. Ind. Eng. Chem. 49, 176.
Hermas, A.A., Morad, M.S., 2008. A comparative study on the corrosion behaviour of 304 austenitic stainless steel in sulfamic and sulfuric acid solutions. Corros. Sci. 50 (9), 2710–2717.
Kalman, E., Varhegi, B., Bako, I., Felhosi, I., Karman, F.H., Shaban, A., 1994. Corrosion inhibition by 1-Hydroxy-ethane-1, 1-diphosphonic acid an electrochemical impedance spectroscopy study. J. Electrochem. Soc. 141, 3357–3360.
Kautek, W., 1988. The galvanic corrosion of steel coatings: aluminum in comparison to cadmium and zinc. Corros. Sci. 28, 173–199.
Kertit, S., Hammouti, B., 1996. Corrosion inhibition of iron in 1M HCl by 1-phenyl-5-mercapto-1,2,3,4-tetrazole. Appl. Surf. Sci. 93, 59.
Kertit, S., Essouffi, H., Hammouti, B., Benkaddour, M., 1998. 1-phenyl-5-mercapto-1,2,3,4-tétrazole (PMT) : un nouvel inhibiteur de corrosion de l'alliage Cu-Zn efficace à très faible concentration. J. Chim. Phys. 95, 2072.
Khadiri, A., Saddik, R., Bekkouche, K., Aouniti, A., Hammouti, B., Benchat, N., Bouachrine, M., Solmaz, R., 2016. Gravimetric, electrochemical and quantum chemical studies of some pyridazine derivatives as corrosion inhibitors for mild steel in 1 M HCl solution. J. Taiwan Inst. Chem. Eng. 58, 552–564.
Khadiri, A., Ousslim, A., Bekkouche, K., Aouniti, A., Warad, I., Elidrissi, A., Zarrouk, A., 2018. 4-(2-(2-(2-(2-(Pyridine-4-yl) ethylthio) ethoxy) ethylthio) ethyl) pyridine as new corrosion inhibitor for mild steel in 1.0 M HCl solution: experimental and theoretical studies. J. Bio-Tribo-Corrosion 4 (4), 64.
Khaled, K.F., 2010. Studies of iron corrosion inhibition using chemical, electrochemical and computer simulation techniques. Electrochim. Acta 55, 6523–6532.
Kowsari, E., Payami, M., Amini, R., Ramezanzadeh, B., Javanbakht, M., 2014. Task-specific ionic liquid as a new green inhibitor of mild steel corrosion. Appl. Surf. Sci. 289, 478–486.
Lee, C.T., Yang, W.T., Parr, R.G., 1988. Development of the Colle-Salvetti correlation-energy formula into a functional of the electron density. Phys. Rev., B. 37, 785–789.
Lgaz, H., Chung, I.M., Salghi, R., Ali, I.H., Chaouiki, A., El Aoufir, Y., Khan, M.I., 2018a. On the understanding of the adsorption of fenugreek gum on mild steel in an acidic medium: insights from experimental and computational studies. Appl. Surf. Sci. 001.
Lgaz, H., Chung, I.M., Albayati, M.R., Chaouiki, A., Salghi, R., Mohamed, S.K., 2018b. Improved corrosion resistance of mild steel in acidic solution by hydrazone derivatives: an experimental and computational study. Arab. J. Chem.
Liu, F.G., Du, M., Zhang, J., Qiu, M., 2009. Corros. Sci. 51 (1), 102–109.
Madkour, L., Elroby, S.K., 2015. Inhibitive properties, thermodynamic, kinetics and quantum chemical calculations of polydentate Schiff base compounds as corrosion inhibitors for iron in acidic and alkaline media. Int. J. Ind. Chem. 6, 165–184.
Mahalakshmi, G., Balachandran, V., 2015. NBO, HOMO, LUMO analysis and Vibrational spectra (FTIR and FT Raman) of 1-Amino 4-methylpiperazine using ab initio HF and DFT methods. Spectrochim. Acta A Mol. Biomol. Spectrosc. 135, 321–334.
Martinez, S., Stern, I., 2002. Thermodynamic characterization of metal dissolution and inhibitor adsorption processes in the low carbon steel/mimosa tannin/sulfuric acid system. Appl. Surf. Sci. 199, 83.
Masroor, S., Mobin, M., Alam, M.J., Ahmad, S., 2017. The novel iminium surfactant p-benzylidene benzyldodecyl iminium chloride as a corrosion inhibitor for plain carbon steel in 1 M HCl: electrochemical and DFT evaluation. RSC Adv. 7, 23182–23196.
McCafferty, E., 2010. Societal aspects of corrosion. Introduction to Corrosion Science. Springer, p. 357.
Moradi, Z., Attar, M.M., 2014. An investigation on the inhibitory action of benzazole derivatives as a consequence of sulfur atom induction. Appl. Surf. Sci. 317, 657–665.
Mu, G., Li, X., Qu, Q., Zhou, J., 2006. Molybdate and tungstate as corrosion inhibitors for cold rolling steel in hydrochloric acid solution. Corros. Sci. 48, 445.
Murulana, L.C., Kabanda, M.M., Ebenso, E.E., 2016. Investigation of the adsorption characteristics of some selected sulphonamide derivatives as corrosion inhibitors at mild steel/hydrochloric acid interface: experimental, quantum chemical and QSAR studies. J. Mol. Liq. 215, 763–779.
Nesic, S., 2007. Key issues related to modelling of internal corrosion of oil and gas pipelines-A review. Corros. Sci. 49, 4308–4338.
Oguzie, E.E., Unaegbu, C., Ogukwe, C.N., Okolue, B.N., Onuchukwu, A.I., 2004. Inhibition of mild steel corrosion in sulphuric acid using indigo dye and synergistic halide additives. Mater. Chem. Phys. 84, 363.
Oguzie, E.E., Lia, Y., Wang, F.H., 2007. Effect of 2-amino-3-mercaptopropanoic acid (cysteine) on the corrosion behaviour of low carbon steel in sulphuric acid. Electrochim. Acta 53, 909–914.
Okafor, P.C., Ikpi, M.E., Uwah, I.E., Ebenso, E.E., Ekpe, U.J., Umoren, S.A., 2008. Inhibitory action of phyllanthus amarus extracts on the corrosion of mild steel in acidic medium. Corros. Sci. 50, 2310–2317.
Öncül, A., Coban, K., Sezer, E., Senkal, B.F., 2011. Inhibition of the corrosion of stainless steel by poly-N-vinylimidazole and N-vinylimidazole. Prog. Org. Coat. 71, 167–172.
Ouakki, Moussa, Galai, Mouhsine, Cherkaoui, Mohammed, Rifi, El-Housseine, Hatim, Zineb, 2018a. Inorganic compound (apatite doped by Mg and Na) as a corrosion inhibitor for mild steel in phosphoric acidic medium. Anal. Bioanal. Electrochem. 10 (7), 943–960.
Ouakki, M., Rbaa, M., Galai, M., Lakhrissi, B., Rifi, E.H., Cherkaoui, M., 2018b. Experimental and quantum chemical investigation of imidazole derivatives as corrosion inhibitors on mild steel in 1.0 M hydrochloric acid. J. Bio Tribo-Corrosion 4, 35.
Parr, R.G., Yang, W., 1989. Density-functional Theory of Atoms and Molecules. Oxford University Press, p. 16.
Quartarone, G., Battilana, M., Bonaldo, L., Tortato, T., 2008. Investigation of the inhibition effect of indole-3-carboxylic acid on the copper corrosion in 0.5 M H2SO4. Corros. Sci. 50, 3467–3474.
Rbaa, M., Galai, M., EL Faydy, M., El Kacimi, Y., EbnTouhami, M., Zarrouk, A., Lakhrissi, B., 2017a. Synthesis, inhibition effects and thermodynamic studies of novel substituted quinolines on the corrosion of mild steel in 1 M HCl solution. J. Mater. Environ. Sci. 8, 3529.
Rbaa, M., Galai, M., El Kacimi, Y., Ouakki, M., Touir, R., Lakhrissi, B., EbnTouhami, M., 2017b. Adsorption Properties and Inhibition of Carbon Steel Corrosion in a Hydrochloric Solution by 2-(4,5-diphenyl-4,5-dihydro-1h-imidazol-2-yl)-5-methoxyphenol. Port. Electrochim. Acta 35 (6), 323–338.
Rbaa, M., Galai, M., Benhiba, F., Obot, I.B., Oudda, H., Ebn Touhami, M., Lakhrissi, B., Zarrouk, A., 2019a. Synthesis and investigation of quinazoline derivatives based on 8-hydroxyquinoline as corrosion inhibitors for mild steel in acidic environment: experimental and theoretical studies. Ionics 25 (7), 3473–3491.
Rbaa, M., Abousalem, Ashraf S., Ebn Touhami, M., Warad, I., Bentiss, F., Lakhrissi, B., Zarrouk, A., 2019b. Novel Cu (II) and Zn (II) complexes of 8-hydroxyquinoline derivatives as effective corrosion inhibitors for mild steel in 1.0M HCl solution: computer modeling supported experimental studies. J. Mol. Liq. 290 (15), 11124.
Salghi, R., Bazzi, L., Hammouti, B., Bouchtart, A., Kertit, S., Ait Addi, Z.A., EL Alami, Z., 2000. Étude électrochimique de l'inhibition de la corrosion de l'alliage d'aluminium 3003 en milieu bicarbonate par les composés triazolique. Ann. Chim. Sci. Mat. 25, 187.
Sasikumar, Y., Adekunle, A.S., Olasunkanmi, L.O., Bahadur, I., Baskar, R., Kabanda, M.M., Obot, B., benso, E.E., 2015. Experimental, quantum chemical and Monte Carlo simulation studies on the corrosion inhibition of some alkyl imidazolium ionic liquids containing tetrafluoroborate anion on mild steel in acidic medium. J. Mol. Liq. 211, 105–118.
Saxena, A., Prasad, D., Haldhar, R., Singh, G., Kumar, A., 2018. Use of Sida cordifolia extract as green corrosion inhibitor for mild steel in 0.5 M H_2SO_4. J. Environ. Chem. Eng. 6 (1), 694–700.
Shaban, S.M., Abd-Elaal, A.A., Tawfik, S.M., 2016. Gravimetric and electrochemical evaluation of three nonionic dithiol surfactants as corrosion inhibitors for mild steel in 1 M HCl solution. J. Mol. Liq. 216, 392–400.
Shahin, M., Bilgic, S., Yilmaz, H., 2002. The inhibition effects of some cyclic nitrogen compounds on the corrosion of the steel in NaCl mediums. Appl. Surf. Sci. 195, 1–7.

Shetty, S.K., Shetty, A.N., 2017. Eco-friendly benzimidazolium based ionic liquid as a corrosion inhibitor for aluminum alloy composite in acidic media. J. Mol. Liq. 225, 426–438.

Shivakumar, S.S., Mohana, K.N., 2012. Cantellaasiatica extracts as green corrosion inhibitors for mild steel in 0.5 M H_2SO_4. Adv. Appl. Sci. Res. 3, 3097–3106.

Singh, A.K., Quraishi, M.A., 2010a. The effect of some bis-thiadiazole derivatives on the corrosion of mild steel in hydrochloric acid. Corros. Sci. 52, 1373–1385.

Singh, A.K., Quraishi, M.A., 2010b. Inhibiting effects of 5-substituted isatin-based Mannich bases on the corrosion of mild steel in hydrochloric acid solution. J. Appl. Chem. 40, 1293–1306.

Singh, S.K., Tambe, S.P., Gunasekaran, G., Raja, V.S., Kumar, D., 2009. Electrochemical impedance study of thermally sprayable polyethylene coatings. Corros. Sci. 51, 595–601.

Singh, A.K., Mohapatra, S., Pani, B., 2016. Corrosion inhibition effect of Aloe Vera gel: gravimetric and electrochemical study. J. Ind. Eng. Chem. 33, 288.

Singh, A., Ansari, K.R., Kumar, A., Liu, W., Songsong, C., Lin, Y., 2017. Electrochemical, surface and quantum chemical studies of novel imidazole derivatives as corrosion inhibitors for J55 steel in sweet corrosive environment. J. Alloy. Comp. 712, 121–133.

Suzuki, T., Nishihara, H., Aramaki, K., 1996. Corros. Sci. 38, 1223–1234.

Tan, B., Zhang, S., Qiang, Y., Guo, L., Feng, L., Liao, C., et al., 2018. A combined experimental and theoretical study of the inhibition effect of three disulfide-based flavouring agents for copper corrosion in 0.5 M sulfuric acid. J. Colloid Interface Sci. 526, 268–280.

Tebhji, K., Hammouti, B., Oudda, H., Ramdani, A., Benkadour, A., 2005. The inhibitive effect of bipyrazolic derivatives on the corrosion of steel in hydrochloric acid solution. Appl. Surf. Sci. 252, 1378–1385.

Verma, C., Olasunkanmia, L.O., Ebensoa, E.E., Quraishid, M.A., 2018. Substituents effect on corrosion inhibition performance of organic compounds in aggressive ionic solutions: a review. J. Mol. Liq. 251, 100–118.

Wang, H.L., Fan, H.B., Zheng, J.S., 2003. Corrosion inhibition of mild steel in hydrochloric acid solution by a mercapto-triazole compound. Mater. Chem. Phys. 77, 655.

Wazzan, Nuha Ahmed, 2014. DFT calculations of thiosemicarbazide, arylisothiocynates, and 1-aryl-2,5-dithiohydrazodicarbonamides as corrosion inhibitors of copper in an aqueous chloride solution. J. Ind. Eng. Chem. 6, 291–308.

Yadav, M., Kumar, S., Sinha, R.R., Behera, D., 2013. Experimental and quantum chemical studies on the corrosion inhibition performance of benzimidazole derivatives for mild steel in HCl. Eng. Chem. Res. 52, 6318.

Yadav, M., Kumar, S., Purkait, T., Olasunkanmi, L.O., Bahadur, I., Ebenso, E.E., 2016. Electrochemical, thermodynamic and quantum chemical studies of synthesized benzimidazole derivatives as corrosion inhibitors for N80 steel in hydrochloric acid. J. Mol. Liq. 213, 122–138.

Zhai, X., Sun, C., Li, K., Agievich, M., Duan, J., Hou, B., 2016. Composite deposition mechanism of 4,5-dichloro-2-n-octyl-4-isothiazolin-3-one in zinc films for enhanced corrosion resistant properties. J. Ind. Eng. Chem. 36, 147.

Zhang, L., He, Y., Zhou, Y., Yang, R., Yang, Q., Qing, D., Niu, Q., 2015. A novel imidazoline derivative as corrosion inhibitor for P110 carbon steel in hydrochloric acid environment. Petroleum 1 (3), 237–243.